Syracuse University Mustangs

Senior Design

(1)

Final Design Review

AEE 472 | Dannenhoffer

Due Date: April 11th, 2019

Michael Aiello, Josh Boucher, Tyler Vartabedian

TABLE OF CONTENTS

NOMENCLATURE

a	=	3D Lift Curve Slope
a_0	=	2D Lift Curve Slope
AR	=	Aspect Ratio
α	=	Angle of Attack
b	=	Wing Span
c	=	Wing Chord
C_D	=	Coefficient of Drag
$C_{D,i}$	=	Lift Induced Drag
$C_{D,0}$	=	Zero-Lift Drag
$C_{D_{SC}}$	=	Discharge Coefficient
C_L	=	Coefficient of Lift
$C_{L,max}$	=	Maximum Coefficient of Lift
$C_{m,CG}$	=	Moment Center of Gravity
D	=	Drag
e	=	Oswald Efficiency Factor
e_0	=	Span Efficiency Factor
g	=	Acceleration of Gravity
H	=	Height of Rocket Bottle
h	=	Height of Water in Rocket
L	=	Lift
m	=	Mass
ρ_{H2O}	=	Density of Water
ρ_{Air}	=	Density of Air
P_∞	=	Pressure
P_N	=	Nozzle Pressure
P_{Tank}	=	Rocket Tank Pressure
q	=	Dynamic Pressure
S	=	Area
R	=	Gas Constant or Diameter of Bottle as Specified

r	=	Diameter of Rocket Nozzle
T	=	Thrust or Temperature as Specified
T_A	=	Thrust Available
T_R	=	Thrust Required
V	=	Velocity
V_N	=	Rocket Nozzle Velocity
V_H	=	Horizontal Tail Area
V_V	=	Vertical Tail Area
V_{LO}	=	Lift Off Velocity
V_{Stall}	=	Stall Velocity
W	=	Weight
ω	=	Turning Rate

LIST OF FIGURES

CHAPTER 2 - INTRODUCTION

2.1 - DESIGN OBJECTIVES

This project calls for the design and manufacturing of a balsa wood, radio-controlled aircraft to be flown in the Carrier Dome on the Syracuse University campus. This aircraft must also externally transport a water-powered rocket while in flight. This water-powered rocket will then be launched from the ground and must remain aloft as long as possible.

Scoring is determined by multiplying the number of laps completed by the rocket's time aloft. This is the only required payload of the aircraft. Optimizing an ideal design will lie within balancing an optimal rocket along without compromising the weight of the aircraft which would then decrease the total laps flown.

2.2 - REQUIREMENTS

The design prompt requires that the aircraft be constructed out of balsa wood and utilize a provided *HBZ3100* radio controlled aircraft components. The rocket must be constructed out of a two-liter soda bottle and powered by water and compressed air. Fins, a nose cone, and a recovery device may be attached with tape but not glue. A parachute may be attached and deployed to increase the time aloft. The nozzle of the two-liter bottle must not be altered.

The aircraft will take off from the end zone of the football field within the Carrier Dome, and must lift off before the 50-yard line. To complete a lap, a figure eight flight path must be flown that follows the outline shown below in *Figure 1*. The aircraft must cross the 50-yard line, turn left around a pylon located at the center of the far 20-yard line, then turn right about a pylon located at the center of the closest 20-yard line, and finally cross the 50-yard line again. This flight path counts for one lap towards scoring. Only one battery may be used on a single charge.

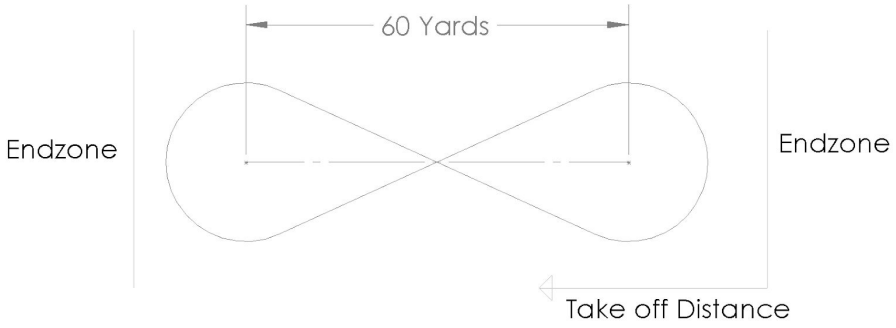

Figure 2.2.1: Flight Path

2.3 - PROJECT TEAM

Team Mustang split work evenly between its three members, specifically delegating tasks and responsibilities based off of individual strengths and weaknesses. Michael Aiello was put in charge of MATLAB coding and optimization of the plane and rocket components. Tyler Vartabedian was tasked with the design and manufacturing of the rocket and aircraft parts as well as keeping the master schedule. Josh Boucher was assigned with formatting the reports and presentations along with assisting in aircraft design and manufacturing.

All decisions were made on a group basis nearing a group consensus. Any difficult or debated decisions were discussed in depth and typically were accompanied by a pros and cons list to assist the group to come to an agreement. Tasks were delegated weekly and followed the Master Schedule shown below in *Figure 3*. Communication occurred daily through both email and a group messaging app. File sharing and editing were performed on the Google-docs platform for ease of editing by every member. Meetings are held three times per week at varying lengths of time.

TYLER VARTABEDIAN

MICHAEL AIELLO

JOSH BOUCHER

Figure 2.3.1: Project Team

2.4 - PROJECT SCHEDULE

The team developed the Gantt chart shown below in *Figure 3* to help maintain appropriate organization and delegate weekly tasks. This chart shows both planned and actual timing for main and subtasks throughout the semester. Note that actual times are not shown for future tasks. This greatly assisted in determining what tasks to be worked on weekly and maintaining a rough timeline for how long each task should take. Anticipating unplanned tasks arising, this note was added into the legend.

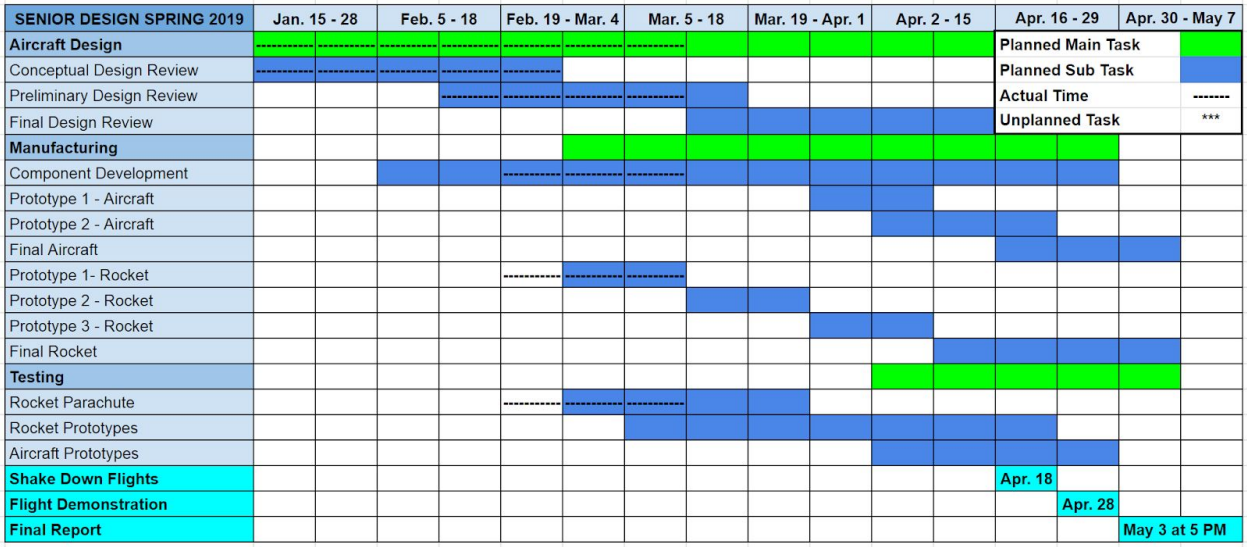

Figure 2.4.1: Planned and Actual Master Schedule

Chapter 3 - Conceptual Design

3.1 - Survey of Existing Designs

Much of the initial design thoughts and ideas for Team Mustang came from observations of prior designs. Specifically, low Reynolds number airfoils were analyzed as well as existing radio controlled aircraft. This led to initial design choices to put towards Figures of Merit for the fuselage, wing type, placement, and angle, tail and propeller configuration, and others.

When searching for low Reynolds numbers airfoils, the assumption of a maximum speed of 20 feet per second was assumed, which coincides with an approximate Reynold's number of 100,000. Three initial airfoils were chosen for analysis, including the Eppler E210, NACA 2412, and Selig S1223.

The Eppler E210 was chosen for its relatively high approximate $C_{L_{max}}$ value at a Reynold's number of 100,000. It also does not feature a complex shape making it structurally sound and easily manufacturable.

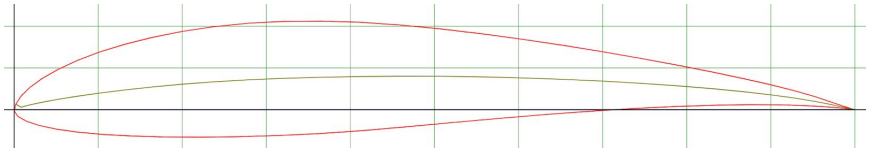

Figure 3.1.1: Eppler E210 Airfoil (3)

The NACA 2412 was also analyzed. Team Mustang has experience analyzing this specific airfoil in prior classes and it was chosen for its proven stability and reliability. With an approximate maximum C_L of only 1.2 at a Reynolds number of 100,000, it has the lowest $C_{L_{max}}$ of the three airfoils analyzed. It is the most structurally simple to manufacture. The NACA 2412 could likely survive a crash if chosen for the aircraft.

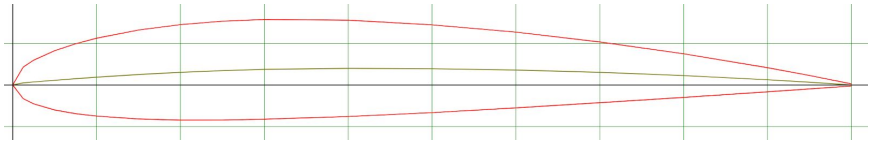

Figure 3.1.2: NACA 2412 Airfoil (8)

The next airfoil analyzed was the Selig S1223. This is by far the best performance airfoil chosen at low Reynolds numbers but features a complex shape making manufacturing difficult. It features a $C_{L_{max}}$ of approximately 2.0 at a Reynold's number of 100,000. The complex shape also makes it susceptible to failure in the event of a crash.

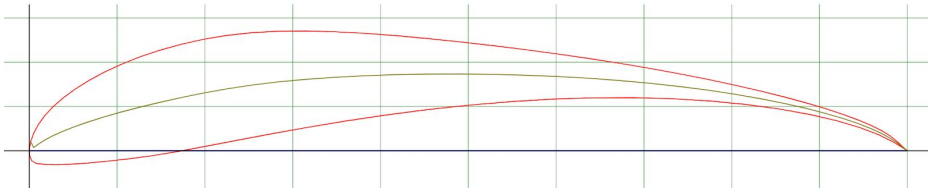

Figure 3.1.3: Selig S1223 Airfoil (10)

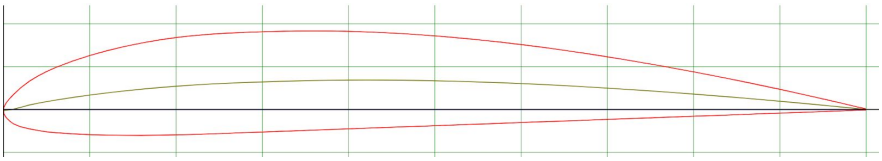

Figure 3.1.4: Clark Y Airfoil (11)

Lastly, the Clark Y airfoil was analyzed. This airfoil was chosen specifically for its flat bottom plate after researching the difficulties associated with applying monokote to an airfoil surface. This airfoil is reliable with the flat bottom surface and a thick camber to allow for structural supports to be inserted while still providing good aerodynamic results.

Radio controlled aircraft models were also analyzed for comparison. *Figure 5* shows the *HBZ3100*, the provided aircraft model for this project. It features a high wing with a conventional fuselage, wing, and tail design. This is a great basis for gauging how the provided electronics from this model will work, however, it does not account for the increased weight with the added bottle rocket. A majority of the surveyed radio controlled planes feature a high and straight wing for a tractor monoplane with a conventional tail.

Figure 3.1.4: HBZ 3100 (6)

Due to the added weight of the bottle rocket, an extremely lightweight design is desirable. Models were analyzed that lack a fuselage to decrease weight, as seen below in *Figure 6.* This specific model utilizes a thin wire as the "fuselage" to reduce weight immensely. Another option includes a half fuselage, which would allow the ease of attachment/storage of the bottle rocket

without the added weight of a fuselage extending to the tail. This would also decrease damage done in the event of a nosedive crash.

Figure 3.1.5: Wire Fuselage Aircraft (5)

Tail design was also closely analyzed. Conventional, T-Tail, H-Tail, cruciform, and V-Tail models were sought out and observed. A vast majority of radio controlled planes utilize the conventional tail configuration. Despite mild interference from the wing, the conventional configuration provides a great balance of stability. The T-Tail, which places the horizontal tail surface at the top of the vertical tail, sacrifices stability but avoids interference from the wing. The cruciform configuration splits the T-Tail and conventional models. V-Tail designs are typically found on fighter aircraft and severely lack stability for more chaotic movement. An H-Tail features a horizontal surface supported by two vertical tail components on each side.

Wing configurations were the last components analyzed. This included elliptical, rectangular, and tapered wing shapes. Elliptical wings are ideal for their performance aspect, decreasing drag while featuring the same aspect ratio as other wings. They are, however, difficult for manufacturing. Tapered wings slightly increase performance but do add some difficulty to manufacturing and structural integrity. Straight wings are featured in a majority of radio controlled aircraft and provide ample stability without manufacturing difficulties.

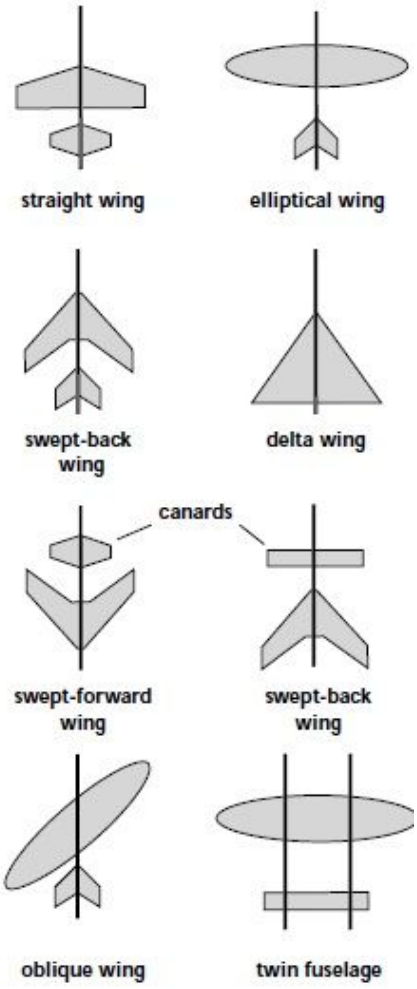

Figure 3.1.6: Configurations (7)

Most radio-controlled aircraft also feature high wing placement, although many still feature mid-level or low placed wings. The high-wing placement is popular due to its great assistance with aerodynamics and ease of manufacturing.
Plus, most heavyweight cargo aircraft feature a high-wing placement, which relates to this projects comparatively heavy payload. Swept wings were also analyzed and considered, but are typically only found on high speed aircraft and add incredible difficulty to manufacturing and production.

Bottle rocket models were analyzed for base design. All models essentially only feature a nose cone and fins attached at the side of the bottle. Some models utilize paper or cardboard nose cones and fins, while others chose to 3D print for more fine-tuned and aerodynamic results at the cost of increased weight. A majority of rockets feature a four fin design for the best stability without enabling too much drag. Many bottle rockets also feature elongated bodies which aids the aerodynamics and stability at the rocket while adding some weight. This can easily be accomplished by slicing a second two-liter bottle and taping it to the top beneath the nose cone. Parachutes are typically attached beneath the nose cone and are made from plastic or paper materials and attached by strings. Some models featured aerodynamically enabled deployment systems for the parachute, while others rely on the nose cone falling off of the rocket so the parachute can deploy.

3.2 - Concept Trade-Offs

Figures of Merit tables were utilized by Team Mustang to choose the baseline design and pertinent configurations. Manufacturability, weight, and performance were the three main aspects analyzed. Low weight and a low profile for decreased drag were sought out, as it is expected the payload bottle rocket will be significantly heavy compared to the weight of the aircraft. A lower weight and drag profile will allow for more laps to be completed leading to a higher score. Each figure of merit table was discussed in depth and voted on by all of Team Mustang and led to an agreeable consensus on each design aspect. The following design aspects were analyzed:

- Aircraft Configuration
- Tail Configuration
- Tail Shape
- Propeller Configuration
- Landing Gear Configuration
- Wing Configuration
- Wing Placement
- Wing Angle
- Fuselage Configuration
- Wing Shape
- Airfoil Type
- Payload Attachment Configuration
- Rocket Fin and Nose Cone Material
- Rocket Parachute Material
- Rocket Parachute Deployment Configuration
- Rocket Body Configuration

Table 3.2.1: Aircraft Configuration						
	Importance	Monoplane	Biplane	Flying Wing	Canard	Dual-Fuselage
Manufacturing	0.2	1	0	0	-1	-1
Drag	0.1	0	-1	1	0	0
Weight	0.3	1	-1	1	-1	-1
Cargo	0.1	0	0	-1	0	-1
Directional Stability	0.3	0	0	-1	1	-1
Total	1	0.5	-0.4	0	-0.2	-0.9

The main considerations when deciding Aircraft Configuration were weight and directional stability. In research, many types of configurations have been successfully used throughout history, but our goal was to decide which would be most likely to succeed given our specific design materials and parameters. With these considerations in mind, a standard monoplane aircraft configuration took the most.

Table 3.2.2: Tail Configuration						
	Importance	Conventional	V-Tail	T-Tail	H-Tail	Cruciform
Manufacturing	0.3	1	0	0	-1	1
Stability	0.3	1	0	-1	1	0
Weight	0.4	0	1	-1	-1	0
Total	1	0.6	0.4	-0.7	-0.4	0.3

In deciding the tail configuration, there were 5 main types that we considered. The least attractive option was the T-Tail, due to the stiffness requirements making the tail extremely heavy, and poor stability. Another poor option we found was the H-Tail configuration. This tail had exceptional stability, but would be very difficult to manufacture, and would most likely be the heaviest option of all. An actually considerable contender for tail configuration was the cruciform. This option is a variation of the T-tail that places the horizontal stabilizer midway down the vertical stabilizer. In turn it is more structurally sound than the T-tail, but still lacks the intended stability we are looking form. The V-tail was the closest second option, but the main disadvantages were the lack of structural stability and difficulty in manufacturing. This left the conventional tail mounted to the fuselage as our best option for the ease of manufacturing, exceptional stability, and average weight.

Table 3.2.3: Tail Shape			
	Importance	Flat Surface	Airfoil
Manufacturing	0.2	1	-1
Performance	0.5	0	1
Weight	0.3	1	-1
Total	1	0.5	03

Table 3.2.3 details the shape of the horizontal tail surfaces. Only a basic analysis was performed at this point in the design project. A flat surface offers the basic elevation requirements with the built in rudders, but does not provide any meaningful lifting forces or stability. This, however, is far easier to manufacture and weighs less. An airfoil profile still gives appropriate elevator parameters while also increasing stability and yielding minor lifting forces thus more greatly improving the aircraft, just at the cost of an increase in difficulty of manufacturing and weight. The provided kit utilizes a flat surface for the tail, enhancing the decision to utilize a flat surface rather than an airfoil profile.

Table 3.2.4: Propellor Configuration			
	Importance	Tractor	Pusher
Manufacturing	0.3	1	-1
Efficiency	0.7	1	0
Total	1	1	-0.3

The main parameter limiting our propulsion system was our single engine capabilities. This limited our options for propeller configurations to tractor and pusher mounted on the fuselage, eliminating the ability for any wing-mounted dual propulsion systems. From research of these two propeller configurations, we found that not only is a pushing configuration more structurally complicated than a tractor, but there is also an increase in drag, and aerodynamic performance suffers from the pusher-type. With these considerations in mind, we chose to

Table 3.2.5: Landing Gear Configuration					
	Importance	Tail Dragger	Tricycle	Bicycle	Quadricycle
Manufacturing	0.3	1	0	0	-1
Toughness	0.3	1	1	-1	1
Weight	0.4	0	0	1	-1
Total	1	0.6	0.3	0.1	-0.4

The four main types of landing gears were analyzed and decided upon. The tail dragger features 2 fixed wheels at the front of the aircraft with a much smaller wheel at the very base of the tail, which gives the aircraft an appearance of dragging its tail on the ground. The tricycle features three fixed wheels at the front of the aircraft, while the bicycle features two wheels along the same axis underneath the center of the fuselage. The quadricycle provides immense toughness at a high weight by featuring four wheels along the front of the aircraft. The tail dragger was picked based off of surveys of existing model aircraft as well as its ease of manufacturing and decent toughness.

Table 3.2.6: Wing Configuration

	Importance	Straight Wing	Delta Wing	Swept Wing	Tapered Wing
Manufacturing	0.2	1	-1	-1	-1
Weight	0.3	1	-1	1	1
Performance	0.3	0	1	1	-1
Toughness	0.2	-1	1	-1	-1
Total	1	0.3	0	0.2	-0.4

When deciding on wing configuration, four major designs used in modern aircraft were considered. The tapered wing configuration is known to be structurally inefficient, and the loads on the wing may be too much for it to handle. Difficult manufacturing process and structural integrity of the wing for a less-than-competitive performance make it a risky choice. The delta wing is strong and efficient, but is very heavy, making it an unattractive choice. The swept wing also has structural integrity issues, but at the benefit of slightly better performance. This makes for a decent second alternative, but the highest scorer was the straight wing configuration, aligning with the “keep it simple” mentality, the straight wing will be easy to manufacture, and will perform fine for our payload mission.

Table 3.2.7: Wing Placement

	Importance	Low Wing	Mid Wing	High Wing
Manufacturing	0.5	1	-1	1
Stability	0.3	-1	0	1
Toughness	0.2	1	0	1
Total	1	0.7	-0.5	1

Wing placement is one of the more important figures of merit analyzed. Manufacturability was weighted highest followed by stability, as the location of the wings in the

event of a crash may prevent or enable catastrophic failure. Survey of existing designs show that largely mobile aircraft feature low dihedral wings, while cargojets feature high anhedral wings. Because the weight of the bottle rocket is expected to be large in comparison to the lifting forces generated by the aircraft, a high wing was chosen. This allows for a lower center of gravity and allows for the bottle rocket to be stored below the aircraft. This specific figure of merit ties in with both the wing angle and payload attachment configuration. A low anhedral wing with cargo attached beneath the airplane would not work, so combining all three into thoughts and ideas yielded the high, straight wing with cargo stored below the fuselage. The high wing allows for ease of manufacturing and keeps the wings stable and secure in the event of a crash.

Table 3.2.8: Wing Angle

	Importance	Dihedral	Straight	Anhedral
Manufacturing	0.4	0	1	0
Stability	0.4	1	0	-1
Maneuverability	0.2	-1	0	1
Total		0.2	0.4	0.2

In continuation of the prior figure of merit table, dihedral wings were essentially automatically eliminated with the choice of a high wing. Straight wings were chosen for the ease of manufacturing, as well as a safety precaution to keep them distanced from the base of the aircraft in the event of a crash. This would prevent any damage to the wings and allow for a faster repair process.

Table 3.2.9: Wing Shape

	Importance	Rectangular	Elliptical
Manufacturing	0.6	1	-1
Weight	0.2	0	1
Lift	0.2	0	1
Total	1	0.6	-0.2

Two wing shapes were analyzed. Elliptical wing shapes provide far better performance with far less drag with the same aspect ratio compared to a rectangular wing, but drastically increase manufacturing difficulty. This was weighted the highest due to concerns over ability to manufacture an elliptic wing efficiently while keeping weight decreased (may require a lot more glue.) Although the performance is greatly increased with elliptical wings, it was deemed it was an unrealistic manufacturing goal.

Table 3.2.10: Fuselage Configuration				
	Importance	Full Balsa	Half Balsa	Full Wire
Manufacturing	0.2	0	-1	1
Weight	0.3	-1	0	1
Cargo	0.3	1	0	-1
Toughness	0.2	1	0	-1
Total	1	0.2	-0.2	0

Three fuselage construction ideas were discussed. A full balsa wood fuselage would extend from the nose to the tail and be entirely made of balsa wood. A full wire fuselage would essentially eliminate a fuselage except for small casings built around the electronics. This wire fuselage would work well if the bottle rocket was elected to be secured as part of the fuselage. The half balsa option is a combination of the other two options, where the first half of the aircraft features a constructed fuselage out of balsa wood, while aft of the wings the fuselage is just a wire connected to the tail. This option reduces weight, slightly, but not as much as the full wire. Here, the ease of storing cargo and the weight were weighted highest while toughness in the event of a crash was considered. A wire fuselage likely would be susceptible to catastrophic failure, while a full balsa wood fuselage could withstand a crash. This is why the full balsa wood fuselage was picked.

Table 3.2.11: Airfoil Type					
	Importance	Eppler E210	Selig S1223	NACA 2412	
Manufacturing	0.3	-1	-1	0	1
Toughness	0.3	1	-1	1	1
Lift	0.4	1	1	-1	0
Total	1	0.7	0.4	0.2	0.7

Arguably the most important figure of merit was to decide the airfoil type to be used in the wings. As explained in section 3.1, three airfoils were analyzed. The Eppler E210 and the Selig S1223 specialize in working with low Reynolds number scenarios, such as what is experienced with radio-controlled aircraft. The NACA 2412 is a very reliable airfoil that has been studied by Team Mustang in prior projects and classes. The S1223 boasts the best performance but features a complex shape that will likely be hard to manufacture an would likely break in the event of a crash. The E210 meets in the middle between the S1223 and NACA 2412, with a simplified profile that could likely withstand a crash and superior performance at low

Reynolds numbers. However, the Clark Y allows for the application of Monokote easily and provides ample performance with a structurally sound profile.

Table 3.2.12: Payload Attachment Configuration				
	Importance	Bottom	Top	Part of Fuselage
Manufacturing	0.3	1	1	-1
Toughness	0.3	0	-1	1
Performance	0.3	0	0	1
Weight	0.1	0	0	0
Total	1	0.3	0	0.3

Three locations for the bottle rocket mounting were considered. This is an essential aspect of the design in order to maintain an appropriate center of gravity without interfering with aerodynamics of the plane. Due to the high wing choice, a bottom mount was initially heavily favored. If a half balsa or full wire fuselage had been selected, making the bottle rocket part of the fuselage would have been an option. This design choice is almost nearly dependent on prior choices, leading to the bottom of the fuselage to be the attachment point for the bottle rocket.

Table 3.2.13: Rocket Nose Cone and Fin Material				
	Importance	Paper	Cardboard	ABS Plastic
Manufacturing	0.2	1	1	0
Toughness	0.4	-1	-1	1
Performance	0.2	0	0	1
Weight	0.2	1	1	-1
Total	1	0	0	0.4

Based off of the survey of prior designs, it was determined that the bottle rocket would feature four fins and a detachable nose cone. It was also observed that these are typically made out of paper, cardboard, or are 3D printed using PLA or ABS plastic. The plastics boast a much higher toughness and resilience to failure when falling back towards the surface after a launch. Although paper and cardboard are incredibly easy to produce and multiple copies of fins and a nose cone could be made, the performance and precision of 3D printing is far superior. The minor increase in weight will be worth the increased aerodynamic properties.

Table 3.2.14: Rocket Parachute Material				
	Importance	Canvas	Plastic bag	Paper
Manufacturing	0.3	0	1	0
Weight	0.3	-1	1	0
Performance	0.4	1	0	0
Total	1	0.1	0.6	0

Three materials were considered for the rocket parachute. Canvas, although a heavy option, is what real parachutes are typically constructed with. Paper is an easily customizable option but lacks the ability to be packed efficiently. A plastic bag is lightweight and packs nicely, but does not perform as well as canvas. Despite this, the plastic bag material was chosen for its ability to pack tightly at a low weight, allowing for a much larger parachute area.

Table 3.2.15: Rocket Parachute Deployment System				
	Importance	Unsecured Nose Cone	Spring Activated	Aerodynamic Activation
Manufacturing	0.3	1	-1	-1
Toughness	0.2	0	1	1
Performance	0.3	0	1	1
Weight	0.2	1	-1	-1
Total	1	0.5	0	0

Multiple designs exist online relating to bottle rocket parachute deployment. Some more advanced models utilize timed spring releases to launch the nose cone off of the rocket so that the parachute can unravel. Others utilize an aerodynamic activation, where the nose cone is dislodged after hitting a certain speed in the rocket. This ultimately just leads to the last option, where the nose cone is simply not restrained to the bottle in any way and is only forced onto the bottle through aerodynamic forces.Both the spring and aerodynamic activation models feature difficult manufacturing techniques and far extra weight. Because of this, the unsecured nose cone option was selected. It does not share the same reliability as the other options, but it should fall off at the tip of the rockets launch and perfectly allow the parachute to deploy.

Table 3.2.16: Rocket Body Configuration				
	Importance	2L Base Bottle	Single Extension	Double Extension
Manufacturing	0.2	1	0	-1
Toughness	0.1	1	0	-1
Performance	0.5	-1	1	1
Weight	0.2	1	0	-1
Total	1	0	0.5	0

Lastly, the rocket body was decided upon. Based off of existing designs, extending the body of the rocket by attaching other two liter bottle bodies increases performance. This, however, increases the weight. Optimization will be required to determine the appropriate length to extend the body. For this project, only one extension will be utilized. This will simply be done by cutting the top of another bottle off and taping it onto the body of the rocket beneath the nose cone and parachute.

3.3 - Baseline Design Configuration

Following the decisions of the Figures of Merit, a baseline design was conceptualized. The aircraft will be a conventional tractor monoplane with a straight, high wing at no angle attached to a full balsa wood fuselage. The tail will be a conventional configuration featuring a straight airfoil profile, most likely a NACA 0012 for its stability, reliability, and ease of manufacturing. A taildragger landing gear system will be utilized. The wings will be rectangular and utilize an Eppler E210 airfoil perfect for low Reynolds number scenarios. This will deliver appropriate lift and stability without compromising ease of manufacturing. Finally, the bottle rocket will be attached below the fuselage by tape or grips or string.

The bottle rocket will feature four attached fins and a loose nose cone 3D printed with ABS plastic. This will provide ample structural integrity to survive falling to the surface after multiple tests. The body of the rocket will be extended by attaching a second two-liter bottle body on top of the initial body. The increased length will increase performance and stability with only a minor cost to the weight. The parachute will be constructed out of a plastic bag and attached via four strings beneath the nose cone. This is a lightweight parachute option that will reliably deploy quickly. The nose cone will not be secured to the body of the rocket, and will simply remain attached due to aerodynamic forces as the rocket rises up. At its peak, the nose cone will fall off thus decreasing the weight and allowing the parachute to deploy effectively.

All balsa wood parts for the aircraft will be laser cut and glued together. Each wing will feature ailerons for great stability and control of the aircraft.

3.4 - Pertinent Equations and Correlations

3.4.1 - Aircraft

When calculating the performance of the aircraft, SLUF was assumed for a majority of the time in air when not performing turns. SLUF, or Straight Level Unaccelerated Flight, is detailed in the following equations:

$$Thrust = Drag = \tfrac{1}{2}\rho V^2 S C_D \quad \textbf{(3.4.1.1)}$$

$$Weight = Lift = \tfrac{1}{2}\rho V^2 S C_L \quad \textbf{(3.4.1.2)}$$

Where ρ is the freestream density, V is the velocity, S is the area of the wing, C_D is the coefficient of drag given by Equation 3.4.1.3 and C_L is the coefficient of lift. The coefficient of lift is directly dependent on the airfoil, angle of attack α, and Reynolds number as seen in Figure 3.4.1.1.

$$C_D = C_{D,i} + C_{D,0} \quad \textbf{(3.4.1.3)}$$

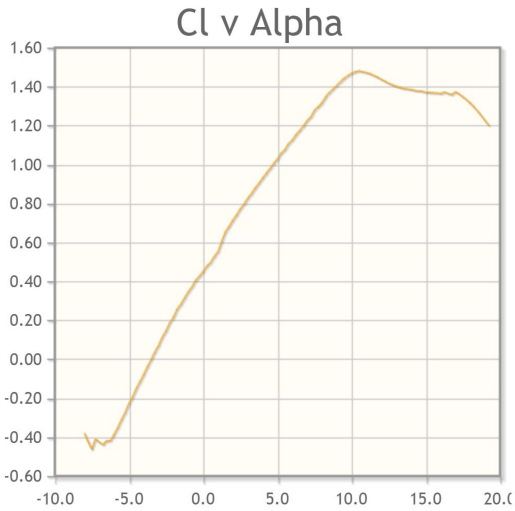

Figure 3.4.1.1: Wire Fuselage Aircraft (3)

Where $C_{D,i}$ is the lift induced drag and is given by Equation 3.4.1.4 and $C_{D,0}$ is the profile drag and is a property of the aircraft as a whole.

$$C_{D,i} = \frac{C_L^{\,2}}{\pi e AR} \quad \textbf{(3.4.1.4)}$$

Where e is the Oswald Efficiency Factor, and AR is the aspect ratio given by Equation 3.4.1.5.

$$AR = b^2/S \quad \textbf{(3.4.1.5)}$$

The Stall Velocity is a very important factor in the aircraft calculations and is given by Equation 3.4.1.6:

$$V_{Stall} = \sqrt{\frac{2W}{\rho S C_{L,max}}} \quad \textbf{(3.4.1.6)}$$

Where W is the weight, and $C_{L,max}$ is a property of the airfoil chosen and is listed under the assumptions. Rate of climb is also important, and is given by Equation 3.4.1.7:

$$R.O.C. = \frac{PA-PR}{W} \qquad \textbf{(3.4.1.7)}$$

Where PA is power available and PR is the power required. These values are given by Equations 3.4.1.8 and 3.4.1.9, respectively.

$$PA = TA \cdot V \quad \textbf{(3.4.1.8)}$$

$$PR = TR \cdot V \quad \textbf{(3.4.1.9)}$$

Where TA and TR are the thrust available and thrust required, respectively. The thrust available is simply the output of the battery as it relates to the given propeller (listed in assumptions), and the thrust required is given by Equation 3.4.1.10:

$$TR = \frac{W}{C_L/C_D} \quad \textbf{(3.4.1.10)}$$

Before rate of climb is considered, liftoff and landing velocities were calculated, and given by Equations 3.4.1.11 and 3.4.1.12, respectively.

$$V_{LiftOff} = 1.2V_{Stall} \quad \textbf{(3.4.1.11)}$$

$$V_{Landing} = 1.3V_{Stall} \quad \textbf{(3.4.1.12)}$$

Performance in the air was also considered when not assuming SLUF. When turning, the following four equations were utilized as they relate to turning and gliding.

$$R = \frac{V^2}{g\sqrt{n^2-1}} \quad \textbf{(3.4.1.13)}$$

$$\omega = \frac{g\sqrt{n^2-1}}{V} \quad \textbf{(3.4.1.14)}$$

$$tan(\theta) = \frac{1}{C_L/C_D} \quad \textbf{(3.4.1.15)}$$

$$R_1 = h \cdot \frac{L}{D} \quad \textbf{(3.4.1.16)}$$

R is the turning radius, ω is the turning rate, θ is the glide angle, h is the height of the aircraft, and R_1 is the glide range. Where g is the acceleration of gravity, and n is the load factor given by Equation 3.4.1.17:

$$n = L/W \qquad \textbf{(3.4.1.17)}$$

Range and Endurance were key towards calculating predicted performance. Range is given by Equation 3.4.1.18 and Endurance is given by 3.4.1.19:

$$R = \frac{\eta}{c}\frac{C_L}{C_D}ln(\frac{W_0}{W_1}) \qquad \textbf{(3.4.1.18)}$$

$$E = \frac{\eta}{c}\frac{{C_L}^{3/2}}{C_D}(2\rho_\infty S)^{1/2}({W_1}^{-1/2} - {W_0}^{-1/2}) \qquad \textbf{(3.4.1.19)}$$

Where η is the propeller efficiency, W_1 is the final weight, and W_0 is the initial weight. Note that these initial and final weights do not factor into this project due to a lack of liquid fuel weight. Similarly important, Power and Thrust Required as they relate to performance can be rewritten as shown in Equations 3.4.1.20 and 3.4.1.21, respectively.

$$(\frac{{C_L}^{3/2}}{C_D})_{max} = \frac{(3C_{D,0}\pi eAR)^{3/4}}{4C_{D,0}} \qquad \textbf{(3.4.1.20)}$$

$$(\frac{C_L}{C_D})_{max} = \frac{(C_{D,0}\pi eAR)^{1/2}}{2C_{D,0}} \quad \textbf{(3.4.1.21)}$$

The prior four equations are the most critical in the performance calculations for the aircraft. Lastly, information about the center of gravity must be calculated to ensure stability. The moment about the center of gravity is given by Equation 3.4.1.22:

$$C_{m_{cg}} = C_{m0} + C_{m\alpha}\alpha + C_{m_{\delta e}}\delta_e \quad \textbf{(3.4.1.22)}$$

And the moment relating to the angle of attack is lastly given by Equation 3.4.1.23:

$$C_{m\alpha} = C_{L_{\alpha w}}(\frac{x_{cg}}{c} - \frac{x_{ac}}{c}) + C_{m\alpha_f} - \eta V_H C_{L\alpha_t}(1 - \frac{d\varepsilon}{d\alpha}) + \eta V_H C_{L\alpha_c}(1 - \frac{d\varepsilon}{d\alpha}) \quad \textbf{(3.4.1.23)}$$

3.4.2 - Rocket

Before any equations for the bottle rocket were derived, a free body diagram expressing the forces on the rocket was drawn, along with labels showing basic dimensions.

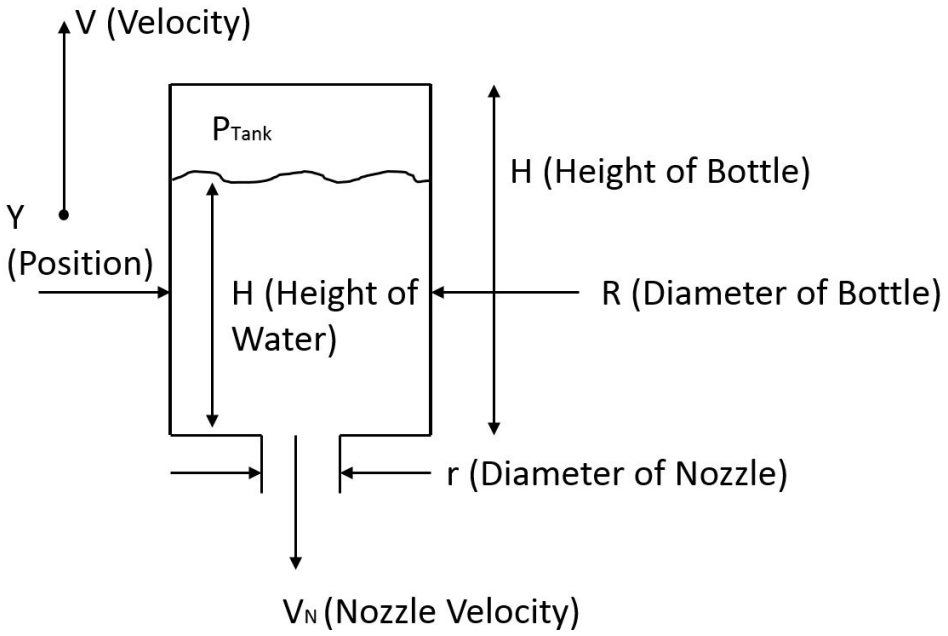

Figure 3.4.2.1: Rocket Free Body Diagram

Firstly, looking at the equations that propel the rocket upwards is the basic thrust equation:

$$T = V_N m_{dot} \quad \textbf{(3.4.2.1)}$$

Where m_{dot} is the mass flow rate and V_N is the velocity of the flow out of the nozzle. This velocity and the mass flow rate are expressed by the following two equations:

$$V_N = C_{D_{SC}}\sqrt{(Pn - P_\infty)/\rho_{H2O}} \quad \textbf{(3.4.2.2)}$$

$$m_{dot} = \rho_{H2O} V_N(\pi/4 \cdot r^2) \quad \textbf{(3.4.2.3)}$$

Where $C_{D_{SC}}$ is the discharge coefficient based on the shape of the nozzle, P_∞ is the exterior pressure, P_N is the pressure in the nozzle of the tank, and ρ_{H2O} is the density of water (the propellent of the bottle rocket.) P_N is expressed in the following equation:

$$P_N = P_{tank} + \rho_{H2O} g h \qquad \textbf{(3.4.2.4)}$$

Where P_{tank} is the pressure of the air within the bottle and is expressed by the following equation:

$$P_{tank}(H-h)A = P_{initial}(H-h_{initial}) \quad \textbf{(3.4.2.5)}$$

Next, the drag and weight must be considered as they act against the thrust. First, the drag is calculated by the following equation:

$$D = \tfrac{1}{2}\rho_\infty V^2 S C_D \qquad \textbf{(3.4.2.6)}$$

Where D is the drag, V is the velocity of the rocket, C_D is the coefficient of drag of the rocket, and S is the area expressed by the following equation:

$$S = \pi(R/2)^2 \qquad \textbf{(3.4.2.7)}$$

Weight also reduces the performance of the rocket and is expressed by the following equation:

$$W = mg \qquad \textbf{(3.4.2.8)}$$

Where m is the mass as expressed by the following equation and g is the acceleration of gravity.

$$m = m_{empty} + \rho_{H2O}(h\pi(R/2)^2) \qquad \textbf{(3.4.2.9)}$$

Lastly, the states need to be expressed in equations, as given by the following three equations for change in height of water, change in velocity, and height of the rocket, respectively.

$$h_{dot} = -m_{dot}/(\rho_{H2O}\pi(R/2)^2) \qquad \textbf{(3.4.2.10)}$$

$$v_{dot} = \Sigma F/m = \frac{T-D-W}{m} \qquad \textbf{(3.4.2.11)}$$

$$y_{dot} = v \qquad \textbf{(3.4.2.12)}$$

3.5 - Assumptions

For the initial conceptual design, basic assumptions were required in many aspects. First, standard day atmospheric conditions were assumed and based on Syracuse Elevation and know statistics about the Carrier Dome. This all corresponds to an approximate elevation of 400 feet for Syracuse, NY. A lack of wind or other aerodynamic disturbances was assumed due to the flights being performed indoors. The other listed assumptions stem from various sources after an extensive amount of research was done to determine approximate values. These values served for the baseline code and performance estimations, and were verified and altered as shown in the following chapter. The following table lists all of the assumptions made for this initial design:

Table 3.5.1: Baseline Values for Assumptions	
Temperature	**288 Kelvin, 14.85 C**
Density	**1.213 kg/m^3**
Pressure	**99,880 N/m^2**
Aircraft Drag Coefficient	**0.075**
Aircraft Thrust	**20 N**
Reynold's Number	**100,000**
Span Efficiency Factor	**0.85**
Oswald Efficiency Factor	**0.85**
Discharge Coefficient of Bottle	**0.7**
Turf Rolling Coefficient	**0.03**
Turf Friction Coefficient	**0.6**
Battery Lifespan	**~120 seconds**
Parachute Drag Coefficient	**1.6**
Bottle Rocket Drag Coefficient	**0.8**
Cruise Velocity of Aircraft	**7.5 m/s**
Lap Length	**125 meters**

On top of this, incompressibility and ideal gas properties were assumed throughout, as well as an instantaneous parachute deployment for the bottle rocket. Changes in air properties were neglected despite an increase in elevation of the aircraft or rocket.

3.6 - Initial Design and Predicted Performance

Utilizing the initial assumptions from Table 3.5.1 and the equations detailed in section 3.4, a predicted final score was determined. Scoring is simply determined by multiplying the number of laps completed by the seconds the bottle rocket remains in the air after launch. This is shown below in Equation 3.6.1:

$$Total\ Score = \Sigma Laps\ Completed \cdot Seconds\ of\ Air\ Time\ of\ Rocket \quad \textbf{(3.6.1)}$$

Figure 3.6.1 shows the expected performance of the rocket, with an expected airtime of 15 seconds. With an estimated lap length of 125 meters and speed of 7.5 meters per second, a lap can be completed in approximately 17 seconds, with extra time built in for turning. This equates to just over seven laps with the assumed battery lifespan. This would lead to an **expected score of 105.**

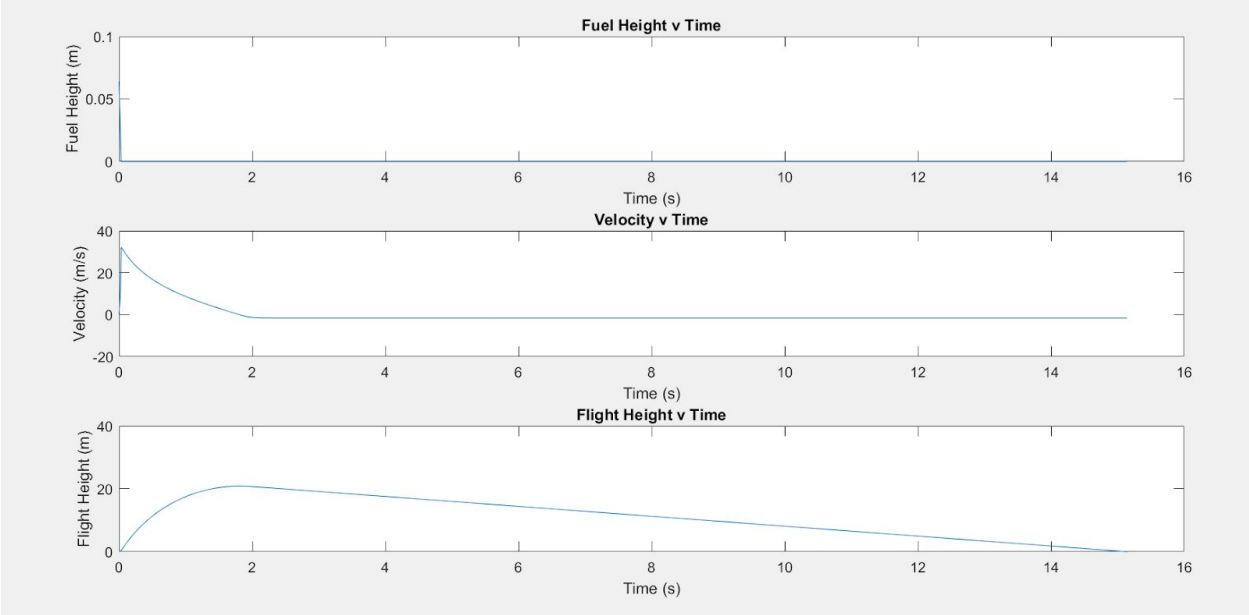

Figure 3.6.1: Rocket Performance Diagram

The results from Figure 3.6.1 are based on the initial water height being set to nineteen percent of the bottle's total height. Running the simulation at this percentage the rocket should be able to achieve a flight height of roughly twenty meters and a flight time, if parachute deploys properly, of fourteen seconds.

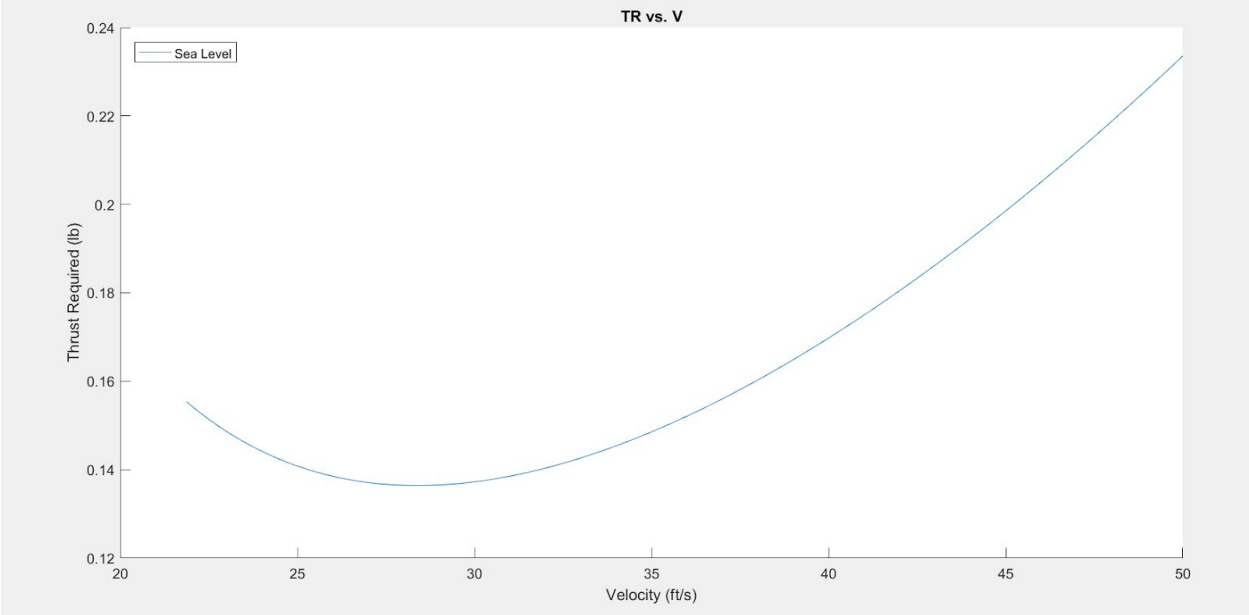

Figure 3.6.2: Thrust Required Aircraft

Figure 3.6.2 depicts the thrust required of the aircraft plotted against its velocity. This graph was obtained from the straight level unaccelerated flight calculations and the stall velocity can be pulled from this graph. The predicted stall velocity is about 21 feet per second.

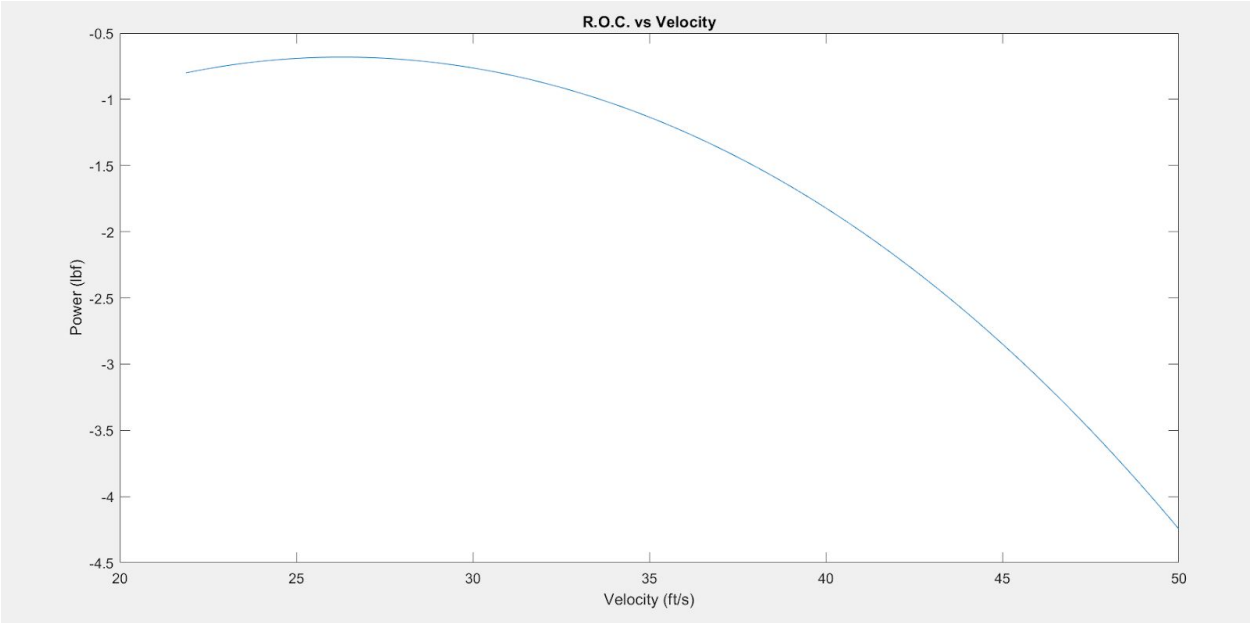

Figure 3.6.3: Rate of Climb Aircraft

Figure 3.6.3 depicts the aircraft's rate of climb as a function of the velocity, the rate of climb is important in regards to power available and power required. Following takeoff, the aircraft will need to climb to a cruise velocity where it will perform the design challenge.

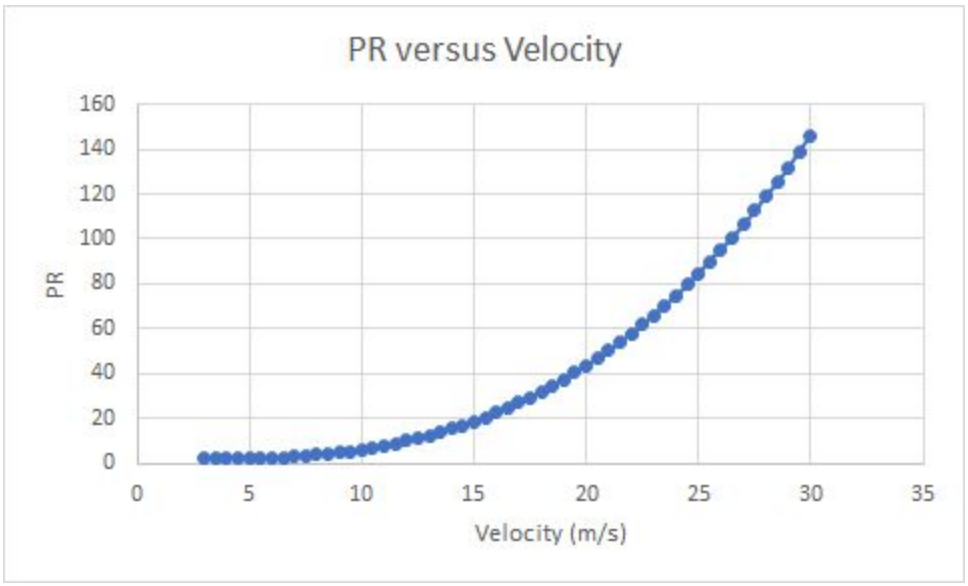

Figure 3.6.4: Power Required for Aircraft at Varying Cruise Velocities

The power required curve is shown in Figure 3.6.4 for varying cruise velocities. This is a critical value to relate to battery aspects and to determine how fast the aircraft can fly given the supplied power.

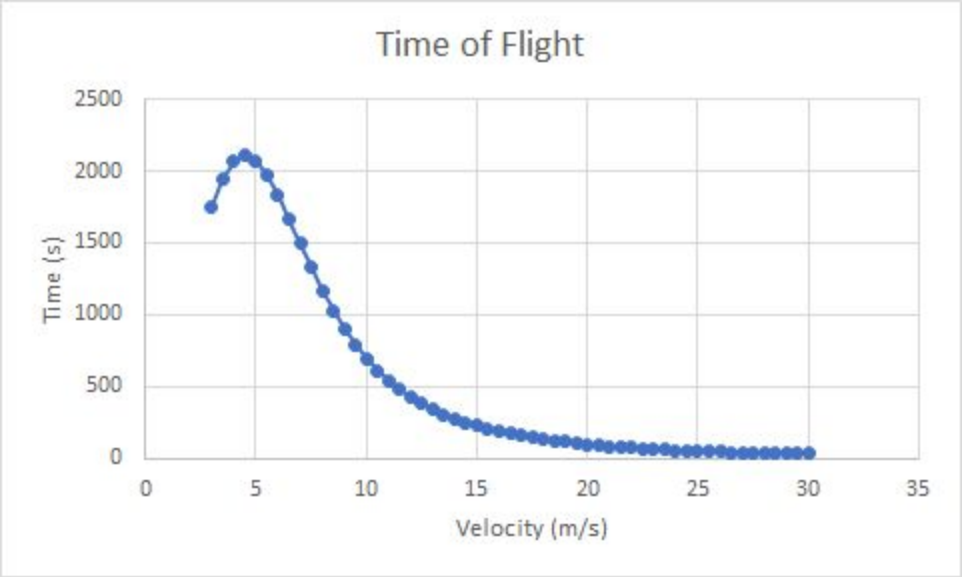

Figure 3.6.5: Time of Flight for Aircraft at Varying Cruise Velocities

Figure 3.6.5 relates the total time of flight for varying cruise velocities. With the initial assumptions, this plot states that for the maximum duration of flight the cruise velocity must be just shy of 5 meters per second, which is just above the stall velocity.

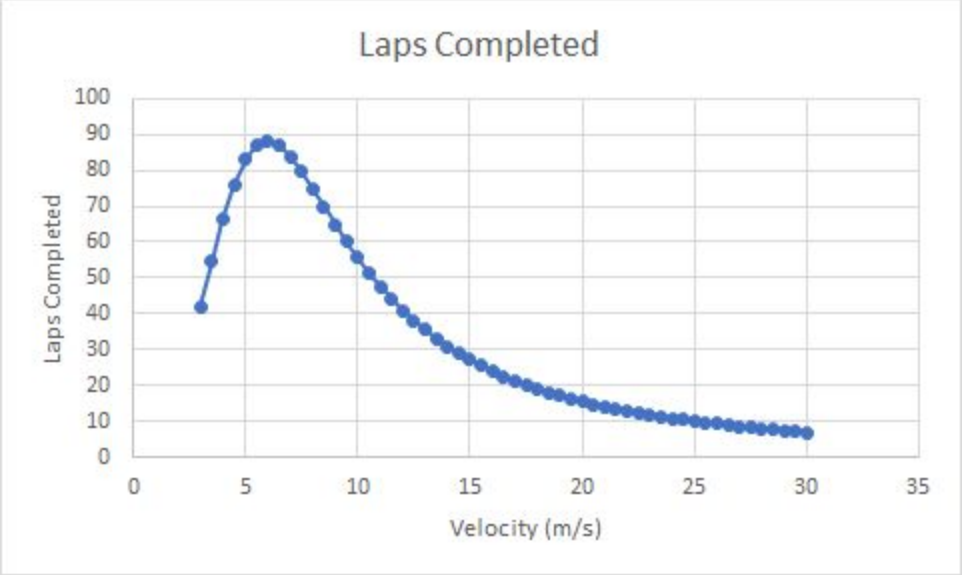

Figure 3.6.6: Laps Completed by Aircraft at Varying Cruise Velocities

Figure 3.6.6 is likely one of the most important data plots created. This shows the total number of laps that could be completed based off of the cruise velocity. This yields an ideal cruise velocity of 6 meters per second. Although the base assumptions will likely change throughout the duration of this project, this plot will be updated to provide an optimization for the most beneficial cruise velocity to maximize score.

3.7 - Sensitivity of Design to Assumptions

Because so many assumptions were utilized in this conceptual design, it can be assumed there is a fair amount of error stemming from calculations. Figure 3.7.1 shows an example as to how small adjustments in assumptions can lead to larger changes in important values, specifically the coefficient of drag for the airplane as a function of altering aspect ratio and Oswald Efficiency values.

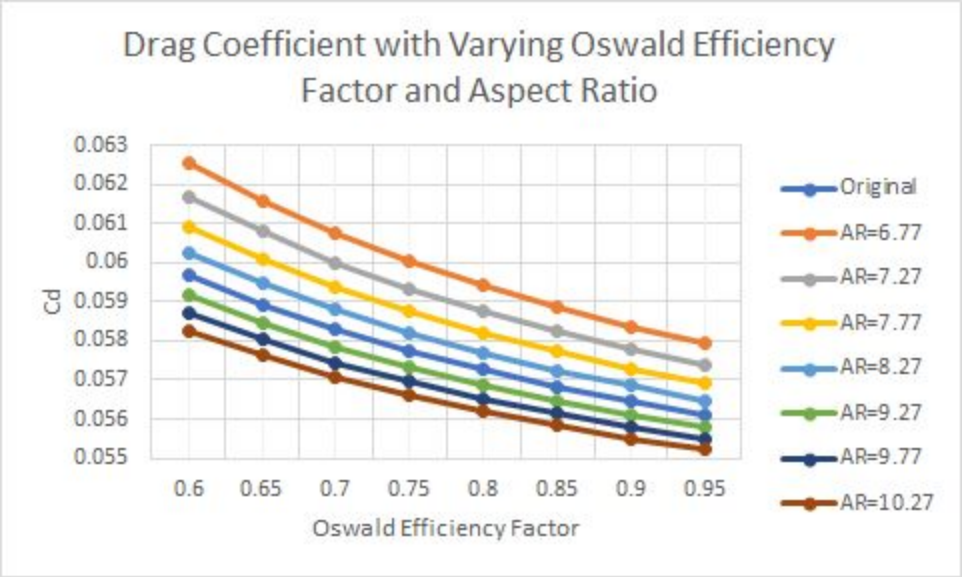

Figure 3.7.1: Drag Coefficient for Aircraft

Figure 3.7.1 plots an Oswald Efficiency Factor varying by 0.5 and an Aspect Ratio varying by the same amount. From the highest to the lowest coefficient of drag, there is a 12% change, with the aspect ratio only changing by 4 and the Oswald Efficiency by 0.35. This is an enormous difference that would factor into predicted performance, optimization, and design, and shows how sensitive initial assumptions can be.

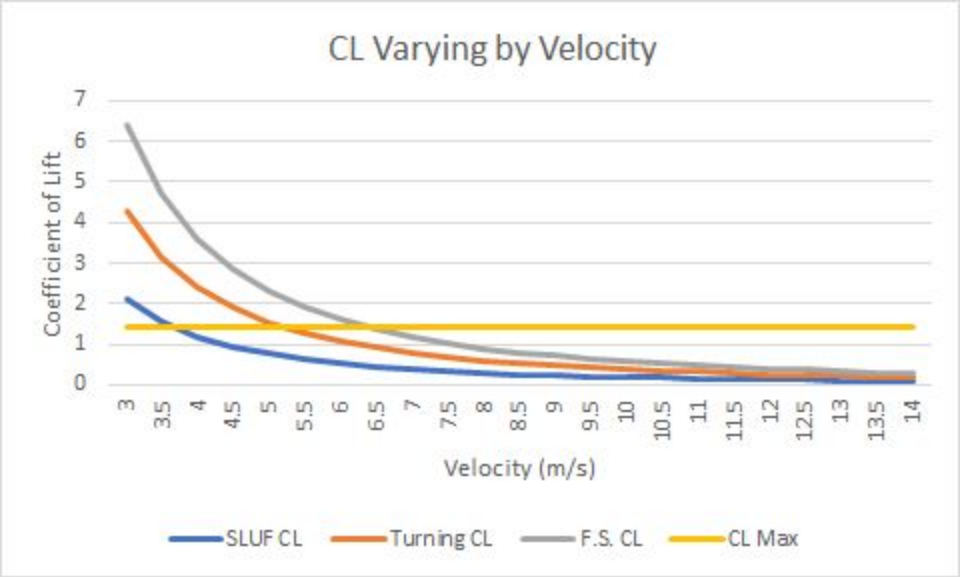

Figure 3.7.2: Varying Lift Coefficients for Aircraft

Figure 3.7.2 shows four coefficients of lifts plotted at varying cruise velocities. This plot shows the sensitivity as to how a coefficient of lift calculation can be altered by assumptions made about the required lift of the aircraft. The "SLUF CL" calculates the lift coefficient strictly by assuming straight, level, unaccelerated flight, equating the lift needed in cruise to the weight exactly. The "TURNING CL" multiples the required lift of the "SLUF CL" by two to account for estimated extra lift required during turning in flight. The "F.S. CL" applies a factor of safety of 1.5 to the "TURNING CL" to assure ample performance. These are all plotted against the maximum lift coefficient of the Clark Y airfoil at a Reynolds number of 100,000 ($C_L = 1.4$). They all converge to approximately the same value as the velocity increases.

Accounting for these large changes is difficult, but the future plan for Team Mustang includes finalizing legitimate values for these assumptions to obtain more accurate results. When assuming a maximum larger lap length (150 m) and a slower cruise velocity at 4.5 meters per second with extra time for turning and take off and landing, this only leads to just over three laps being flown by the aircraft rather than the initial seven. This results in a final score of only 45 points, 42% of the original estimate. If the rocket air time is also reduced by five seconds, the final score is reduced to 30 points, just 28% of the initial estimated score. These ranges are incredibly large due to the uncertainties of the assumptions. This will be changed in the following Preliminary Design Review, where tests will be performed to achieve legitimate data values to improve performance predicting code and optimization of the aircraft and rocket.

Chapter 4 - Preliminary Design

4.1 - Verification of Critical Assumptions

Before finalizing the design of the aircraft and payload, Team Mustang performed various tests to verify critical assumptions. Many assumptions still remain in place due to our aircraft not being constructed, such as the profile drag. These assumptions were still complemented by other tests and more intense research to determine more legitimate values. Team Mustang specifically participated in a variety of tests while teaming together with other teams to determine official values for critical assumptions. Table 4.1.1 shows all of the tested critical assumptions and reaffirmed assumptions.

Table 4.1.1 - Verification of Critical Assumptions of Aircraft

Variable	New Value	Initial Value	Percent Change
Turning Radius (m)	8	10	-20%
Lap Length (m)	178	125	43%
Cd 0*	0.05	0.075	-33%
CL Max*	1.3	1.4	0%
CL 0*	0.3	0.4	-25%
Cruise Velocity (m/s)	6	10	-40%
Mass (kg)*	2.192	1.4	57%
Rolling Coefficient	0.05	0.03	66%
Oswald Efficiency*	0.8	0.85	-6%
Battery Efficiency	0.8	N/A	0%
Motor Efficiency	0.22	N/A	0%
Max Thrust (N)	5.886	20	-71%
Mass of Aircraft Comp.	352	N/A	0%
Battery Lifespan Max Thrust (s)	360	120	200%
Max Current	14	18	-22%
Empty Mass of Rocket (kg)	0.112	0.042	166%
Total Rocket Mass (kg)	0.372	0.102	264%
Rocket Body Cd	0.45	0.8	-44%
Parachute Cd	0.68	1.6	-58%
Discharge Coefficient	0.84	0.7	20%
Reynolds Number	80419	100,000	-19%

**Values just updated - not verified by a test, only primary research.*

To bring this table together, Team Mustang participated in various rocket parachute tests to determine parachute coefficients of drag, a battery stress test to determine the degradation of maximum thrust available over time, the lifespan of the battery at maximum thrust, the current supplied at max thrust over time, the current at various throttle ticks, and the discharge coefficient of the rocket. The following images show some of the tests being performed and the equipment used.

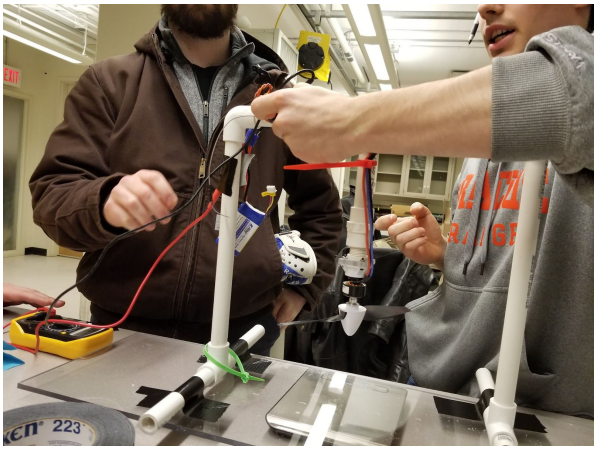

Figures 4.1.2 (Top Left), 4.1.3 (Top Right), 4.1.4 (Bottom Left), 4.1.5 (Bottom Right) - Verification of Assumptions

Figure 4.1.6 below shows the results from the battery and thrust tests. For the first two top plots, current and thrust were measured at each throttle tick on the controller. This utilized a PVC pipe apparatus securing the motor and propeller pointed down all on top of a weight scale. The negative weight from the scale was recorded as the thrust and plotted. This is shown in Figure

4.1.4. The current was recorded at each tick mark twice. The same PVC apparatus was used for the bottom two plots, where the battery was recharged, then the throttle was set to maximum. The thrust value decreased over time proportionally to the decreasing current over time.

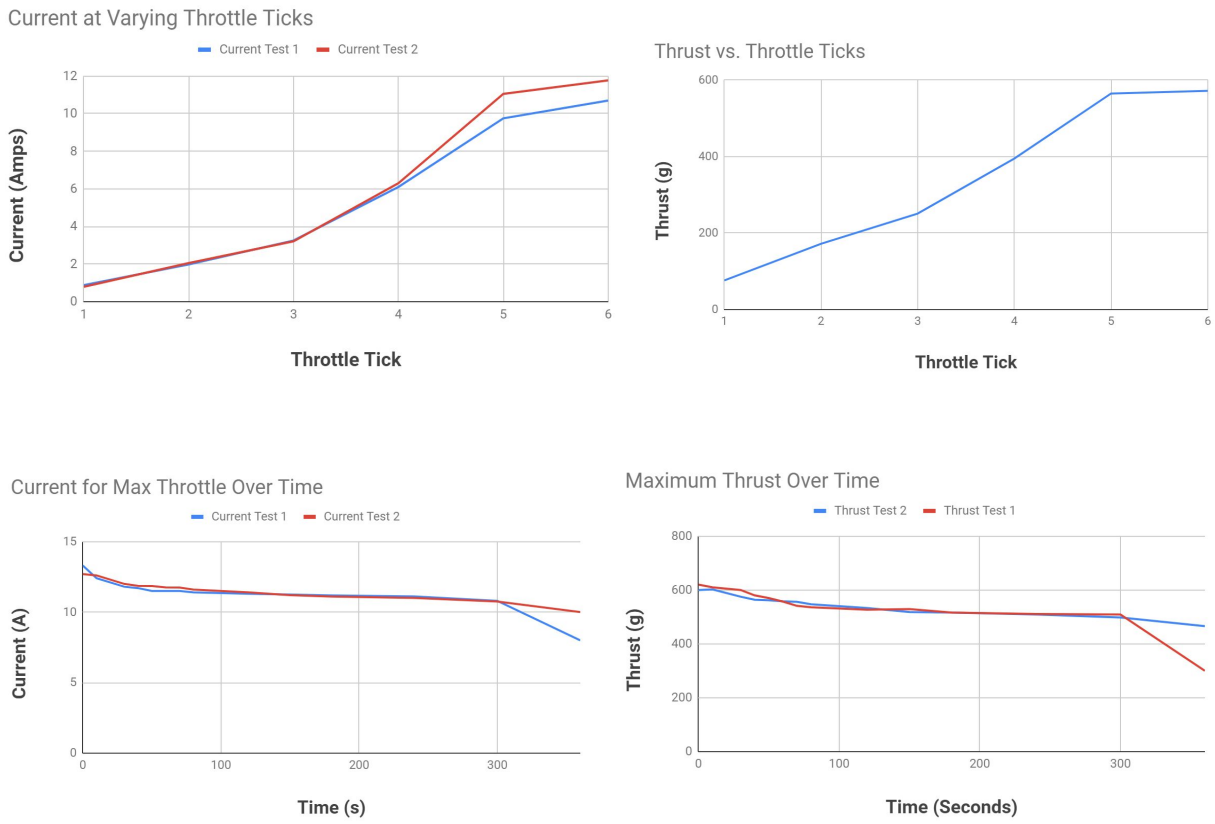

Figure 4.1.6 - Current and Thrust Test Results

Note that the Reynolds number calculated in Table 4.1.1 is calculated through Equation 4.1.1:

$$Re = \rho vc/\mu \qquad \textbf{(4.1.1)}$$

4.2 - Overall System Design

The base aircraft design will utilize the provided electronics and motors from the HBZ3100 kit provided. These components make up the majority of the system design, while the fuselage, tail, and wings will be constructed out of laser cut balsa wood. The provided landing gear from the kit will also be utilized. Various 3D printed parts will assist in the design. For the rocket design, a 3D printed nose cone and fins will be attached to the rocket body, with pieces of other two liter bottles assisting the designs performance. A canvas 24 inch parachute will be taped to the top of the 2 liter bottle under the nose cone. Each piece with the corresponding masses of every part are shown in Table 4.2.1:

Table 4.2.1 - System Parts and Masses	
Part	**Mass (g)**
Rocket Nose Cone	36.5
Rocket Fins	20
Rocket Tape	5
Rocket Parachute	6
Rocket Body	45.5
3 Control Surface Servos	76
Motor	115
Battery	95
Electronic Receiver and Transmitter	11
Landing Gear	30
Screws, Mounts, Rubber Bands	25
TOTAL ROCKET	**113**
TOTAL AIRCRAFT	**386.5**
TOTAL COMBINED (without water)	**499.5**

Each of the electronic aircraft components will be connected by wires throughout the fuselage. The transmitter will be encased and secured to a 3D printed case behind the wings to minimize drag. The Motor will be screwed into a 3D printed mount built into the fuselage. The three servos included for the three control surfaces will be mounted on the fuselage close to their respective control surface. Wire extensions may be required depending on the final length of the fuselage. The landing gear will be secured into a 3D printed mount in the fuselage just below the wing. The rocket will feature four fins and a nose cone all 3D printed and rest partly in the fuselage and partly below the wings.

4.3 - Wing Aerodynamic Design

As discussed in prior sections, the wing will be a straight, rectangular, high wing comprised of a Clark Y airfoil. The Clark Y airfoil was again chosen for its reliable performance and the flat bottom which will work appropriately with a monokote application. Here, obviously, the focus is on ease of manufacturing. Further optimization was performed to determine the chord, span, and aspect ratio. This optimization was performed using Excel and the results are shown below in Figure 4.3.1:

Laps Completed

ASPECT RATIO	CHORD (METERS)																			
7.8	2.026956	3.0448	4.340569	5.928759	7.807622	9.953451	12.31582	14.81574	17.34883	19.79455	22.0308	23.95066	25.47687	26.57	27.22881	27.48378	27.38696	27.00118	26.39109	25.61692
7.6	1.924954	2.892472	4.125524	5.639486	7.435277	9.494079	11.77269	14.20123	16.685	19.11185	21.36474	23.337	24.94665	26.14573	26.92264	27.29784	27.31518	27.0319	26.50962	25.80762
7.4	1.825523	2.743874	3.91548	5.356388	7.069829	9.041376	11.23449	13.58785	16.01623	18.41615	20.67641	22.69187	24.37721	25.67702	26.56992	27.0663	27.20133	27.02586	26.59769	25.97448
7.2	1.728674	2.599028	3.710496	5.079598	6.711542	8.595819	10.70197	12.97672	15.344	17.70909	19.96736	22.01636	23.7688	25.16306	26.16873	26.78625	27.04173	26.97898	26.65113	26.11348
7	1.634412	2.457956	3.510628	4.809241	6.36067	8.157869	10.1759	12.36898	14.66979	16.99243	19.23934	21.31184	23.12203	24.60339	25.71738	26.45488	26.8327	26.88699	26.66543	26.22019
6.8	1.542745	2.32068	3.315929	4.545437	6.017457	7.727977	9.657034	11.76574	13.99514	16.26799	18.49426	20.57993	22.43783	23.99788	25.21451	26.06957	26.57056	26.74546	26.63578	26.28974
6.6	1.453679	2.187218	3.12645	4.288302	5.682139	7.306574	9.146094	11.16814	13.3216	15.53772	17.73421	19.82255	21.7175	23.34683	24.65913	25.62798	26.25174	26.54989	26.5571	26.31686
6.4	1.367222	2.057591	2.942239	4.037945	5.354937	6.894079	8.643796	10.57728	12.65073	14.80358	16.96144	19.04189	20.96275	22.65099	24.05071	25.12812	25.87286	26.29577	26.42412	26.29585
6.2	1.283379	1.931815	2.763342	3.794469	5.036067	6.490894	8.150829	9.994237	11.98409	14.06764	16.17834	18.24039	20.17563	21.91159	23.3892	24.56845	25.43086	25.97868	26.23138	26.2207
6	1.202156	1.809908	2.589801	3.557972	4.725731	6.097401	7.66786	9.42009	11.32326	13.33198	15.38743	17.42075	19.35862	21.13037	22.67515	23.94797	24.92307	25.5944	25.97342	26.08505
5.8	1.123558	1.691884	2.421656	3.328547	4.424121	5.713969	7.195533	8.855873	10.66977	12.5987	14.59133	16.58589	18.51458	20.3096	21.90973	23.26633	24.34738	25.13907	25.64485	25.8824
5.6	1.04759	1.577759	2.258946	3.106281	4.131419	5.340945	6.734464	8.302596	10.02515	11.86994	13.79276	15.73895	17.64671	19.45209	21.0948	22.52391	23.70235	24.60934	25.24054	25.60615
5.4	0.974257	1.467547	2.101706	2.891255	3.847799	4.978661	6.285244	7.761232	9.390893	11.14781	12.99449	14.88324	16.75858	18.56121	20.23292	21.72192	22.98739	24.00255	24.7558	25.24986
5.2	0.903562	1.361259	1.94997	2.683547	3.573419	4.62743	5.848432	7.232718	8.768457	10.43442	12.19933	14.02222	15.85408	17.64081	19.32739	20.86245	22.20283	23.31693	24.18662	24.8074
5	0.835511	1.258909	1.803767	2.483228	3.308433	4.287545	5.424562	6.717951	8.159252	9.731835	11.41011	13.15948	14.93736	16.69529	18.38224	19.94857	21.3501	22.55175	23.52988	24.27329
4.8	0.770106	1.160508	1.663126	2.290365	3.052981	3.959284	5.014134	6.217783	7.564633	9.04208	10.62965	12.29868	14.01281	15.72945	17.40224	18.98429	20.43182	21.7076	22.78367	23.64296
4.6	0.707352	1.066064	1.528075	2.10502	2.807195	3.642903	4.617621	5.733022	6.985901	8.367118	9.860732	11.4435	13.08501	14.74853	16.39283	17.97467	19.45187	20.78646	21.94751	22.9131
4.4	0.64725	0.975589	1.398638	1.927249	2.571195	3.338642	4.235464	5.26443	6.424291	7.708842	9.106087	10.59765	12.15865	13.75808	15.36008	16.9257	18.41544	19.79193	21.02265	22.08208
4.2	0.589805	0.88909	1.274837	1.757105	2.345095	3.046724	3.868073	4.812719	5.880972	7.069059	8.368363	9.764797	11.23849	12.76392	14.31058	15.84429	17.32905	18.72929	20.01227	21.15026
4	0.535019	0.806575	1.156693	1.594637	2.128998	2.767353	3.515828	4.378554	5.357041	6.44949	7.65011	8.948517	10.32932	11.77204	13.2514	14.73817	16.20047	17.60553	18.92168	20.12036
3.8	0.482894	0.728052	1.044224	1.439888	1.922997	2.500717	3.179079	3.962549	4.853522	5.851751	6.95376	8.15229	9.435856	10.78851	12.18991	13.61576	15.03865	16.42937	17.7584	18.99774
3.6	0.433433	0.653527	0.937448	1.292898	1.727179	2.246986	2.858145	3.56527	4.371364	5.277356	6.281614	7.379452	8.562699	9.819397	11.13369	12.48602	13.85355	15.2111	16.53222	17.79057
3.4	0.386637	0.583006	0.83638	1.153704	1.54162	2.006317	2.553319	3.187234	3.911437	4.727706	5.635825	6.633166	7.714299	8.87067	10.0904	11.35827	12.65595	13.96247	15.25502	16.50991
3.2	0.342508	0.516494	0.741034	1.022337	1.366391	1.778847	2.264863	2.82891	3.474538	4.20409	5.018389	5.9164	6.894889	7.94812	9.067614	10.24203	11.4572	12.69636	13.94061	15.16957
3	0.301048	0.453997	0.651421	0.898826	1.201554	1.564703	1.993012	2.490719	3.061384	3.707677	4.431138	5.231907	6.108446	7.057274	8.072723	9.146775	10.26898	11.42651	12.6044	13.78591
2.8	0.262258	0.395517	0.567553	0.783197	1.047163	1.363995	1.737976	2.173037	2.672619	3.239526	3.875737	4.582209	5.358658	6.203331	7.112801	8.08178	9.102996	10.16714	11.26295	12.37733
2.6	0.22614	0.341059	0.489439	0.675471	0.903268	1.176819	1.49994	1.876197	2.308816	2.800576	3.353676	3.969588	4.648893	5.391104	6.194494	7.055929	7.970727	8.932567	9.933451	10.96374
2.4	0.192693	0.290626	0.417088	0.57567	0.769909	1.003261	1.279065	1.600489	1.970474	2.391657	2.866278	3.39608	3.982187	4.624974	5.323937	6.07755	6.883142	7.736791	8.633242	9.565878
2.2	0.161921	0.24422	0.350506	0.483808	0.647123	0.843394	1.075489	1.346164	1.658028	2.01349	2.414699	2.863475	3.361227	3.908859	4.506679	5.154289	5.850484	6.593159	7.379217	8.204514
2	0.133822	0.201844	0.289699	0.3999	0.53494	0.697279	0.88933	1.113436	1.371848	1.666692	1.999932	2.373321	2.788353	3.246199	3.747642	4.293006	4.882075	5.514025	6.187343	6.899766
	0.0762	0.08739	0.09858	0.10977	0.12096	0.13215	0.14334	0.15453	0.16572	0.17691	0.1881	0.19929	0.21048	0.22167	0.23286	0.24405	0.25524	0.26643	0.27762	0.28881

Figure 4.3.1 - Aerodynamic Optimization

Here, a varying chord is plotted against the aspect ratio while the span varies. The chord length varies from 0.0762 meters (3 inches) to 0.28881 meters (1 foot). The aspect ratio varies from 2 to 7.8. The cells each calculate the number of laps completed using the calculated cruise velocity of 6 meters per second and other variables. The best values are seen in the reddish hue, while the worst values are seen in green. Obviously, the higher the aspect ratio, the better the performance. However, the larger aspect ratios will be limited by the structural integrity of a longer span. This specific optimization yields a chord length of 0.24405 meters, and an aspect ratio of 7.8, which yields a span of 1.9 meters. This would allow for over 27 laps to be completed, leading to a total score of 405 with the current rocket airtime of 15 seconds. If a more realistic span of about 1 to 1.5 meters is chosen, 23 laps can be completed at the same ideal chord of 0.24405 meters and an aspect ratio of 6, which yields a span just shy of 1.5 meters. This determination falls in the optimization of the wing structural design. In a future model of this optimization, it will account for takeoff and other aspects. This optimization largely depends on cruise velocity, lap length and proportionally turning radius, profile drag, and the weight of the aircraft. An end goal for this optimization will also account for an increase in weight as the span and aspect ratio increases, and simultaneously optimizing that while meeting the structural integrity requirements and maximizing the performance.

A decision on the location of ailerons was also made. It was decided that they would be placed as close to the outer edges of the wings as possible to increase their impact on stability.

4.4 - Wing Structural Design

With the wing aerodynamic optimization calling for a high aspect ratio and a span potentially exceeding 1.5 meters, structural optimization is critical. The wing is a simple straight rectangle, allowing for an easier structural analysis. This specifically will optimize weight versus span, limiting the aspect ratio and allowing to achieve the best aerodynamic results. This will

also optimize the size of the supporting wing spars, number of spars, and the number of airfoil ribs in each wing. Each wing will be attached to the fuselage via a 3D printed mount. This allows for ease of customization around the rocket bottle which will be a part of the fuselage. If allowed, the ribs will be cut out of foam, supported by carbon fiber spars. Ideally three spars will be utilized, with two in the middle on the top and bottom of the ribs, and then one more at the front. This will give maximum survivability in the event of a crash. The wings and spars will fit into 3D printed mounts glued into the fuselage.

If carbon fiber spars are used, this will likely limit customization and optimization of the sizes as McMaster-Carr only sells three sizes of square carbon fiber tubes. This would also eliminate the need for structural analysis of wing loading (excluding optimizing the number of ribs) because any forces experienced by the aircraft in flight would not nearly lead to any type of failure in the supporting struts as the tensile and compressive strength of carbon fiber is enormous. If balsa wood is used, this opens up potential to customize the sizing, as a long piece of balsa wood could be laser cut into conceivably any size and shape. However, the balsa wood is not structurally sound and could lead to catastrophic failure in the event of a crash. It is lightweight and cheap, but if the wing spars break in a crash, it is likely that the wings will not be salvageable. More research into options available to purchase for both materials needs to be done before determinations on structural aspects can be made.

Early structural determinations based on a lot of assumptions are calling for an estimate of 8 ribs per wing for 16 ribs in total, along with the 3 wing spars mentioned prior for each wing to hold each rib together. For the final design review, ribs will be made out of both foam and balsa wood and weighed along with the spars to allow for a more accurate weight prediction. The wings will be covered with monokote and constructed out of balsa wood and glue to secure the wood together.

4.5 - Fuselage Structural Design

The fuselage, that will be constructed entirely out of balsa wood, will feature three bulkheads. The first bulkhead will be located at the front of the fuselage to mount the motor and secure the components of the propeller. The remaining two bulkheads will be located before and after the wing to provide structural stability. Stringers, also made of balsa wood, will be placed along the high stress areas of the fuselage to stiffen the structure and prevent catastrophic damage in the event of the crash. The belly of the fuselage will be open. The purpose of having an open belly fuselage is to secure fifty percent of the payload within the aircraft and the other fifty percent of the payload will be outside the aircraft. The goal is to design the fuselage so that it hugs the payload tightly and that it will be able to slot in airtight. The advantages of having the fuselage encompass the payload are that drag will be significantly reduced when flying and that a standard tricycle landing gear system can be used without requiring an abnormal clearance height.

4.6 - Payload System Design

Rocket Design

The payload that is to be carried by the aircraft for the entire duration of its flight is a 2-liter bottle (“rocket”). The goal is to build a rocket that can stay aloft for the longest period of time, the original bottle cannot be altered in anyway. Team Mustang will be adding four components to the original rocket to maximize time aloft. The first attachment is a 3D printed nose cone. When the pressurized rocket is launched the nose cone will reduce drag which will allow for the rocket to achieve its maximum height. In addition to the nose cone the rocket will also feature three 3D printed fins to increase aerodynamic performance. Both the nose cone and fins were 3D printed to save on weight without compromising structural stability. In the photo below, on the right, you can see the nose cone and fins and how they will be attached to the rocket.

Figure 4.6.1 - Rocket Prototype 1 and Parachute Options

Third, we plan to take a second 2-liter bottle which will be cut in half, and the top half of the cut bottle will be slid onto the original rocket. This will extend the overall length of the rocket and provide a more stable flight. The last attachment to the rocket that will help increase time aloft is the addition of a parachute. The parachute will be folded up and located under the nose cone. In theory, once the rocket stops accelerating upwards and gravity takes control, the nose cone will detach allowing the parachute to unfold and inflate. Two parachutes were tested, both are featured in the photo above on the left. The blue checkered parachute is 18 inches and made of plastic where the red parachute is 24 inches and made of nylon. Although the nylon is heavier

than plastic it was able to inflate better after being folded and was aloft longer. The red parachute is larger which will increase drag during the rockets descent increasing the time aloft.

4.7 - Propulsions System Design

Propulsion

Team Mustang's aircraft will be powered by a single motor with the propeller fixed as a tractor opposed to a pusher orientation. The motor selected for the aircraft is that of the original HBZ3100 kit, we will be flying with the 370 BL Motor, with 1300Kv and three 3.5mm bullet connectors. This single prop aircraft will be required to sustain itself during flight as well as carry the rocket payload. To provide the best performance the aircraft is expected to cruise around 6 m/s with a stall velocity of around 3.3 m/s. The power required of the aircraft was determined by taking the thrust required multiplied by velocity and dividing that by power of the battery, further this quantity was then divided by the efficiency of the battery. The power available of the aircraft was determined through experimental testing. The motor is powered by a 1300mAh 3S 11.1V 20C LiPo battery that will be situated in the fuselage of the aircraft.

Structural Design

The propeller will be located at the front of the aircraft in tractor orientation. Components of the HBZ3100 kit will be implemented for stability and aerodynamic profile. The power components will largely be located in the fuselage, with the motor shaft and the motor more likely to be in the nose of the aircraft. The propulsion system will constructed in the same manner as the HBZ3100 kit with the plastic cowl and spinner supporting the propeller. To adhere the plastic component to the balsa wood frame a cyanoacrylate glue will be used. The glue ("Super Glue") was chosen instead of an epoxy because of its advantageous adhesive properties. Another reason for the selection of a glue is that come flight day in the event of a crash, it will be faster to make any repairs with a super glue opposed to an epoxy.

Controls

Two types of servos will be featured in the aircraft. The first, being, the SV80 Long Lead Servo that will run through the nose of the aircraft to provide power to the propeller. The second, being, the DSV130 3-Wire Digital Servo Metal Gear which will provide power to the elevator on each wing and rudder on the tail.

Radio Control

A DXe DSMX transmitter will be used for the aircraft. The transmitter operates on a bandwidth of 2.4 GHz. The transmitter supports three flight modes and is powered by four AA alkaline batteries. Most likely the two most important pre-programmed features of this radio

controller are the specific channels for throttle, elevator, and rudder, as well as the bind/panic/return home button for safe flight and retrieval of the aircraft.

4.8 - Tail Design

Due to a largely high payload mass comparable to the aircraft mass, stability and the ability to quickly return to an equilibrium cruise is crucial. This is why the tail design is absolutely essential. Source #13 from the Massachusetts Institute of Technology details that typical ranges of horizontal and vertical tail aspects in radio controlled aircraft are as shown below:

$$0.3 \leq V_H \leq 0.6$$

$$0.02 \leq V_V \leq 0.05$$

Where V_H is the horizontal tail volume coefficient and is given by Equation 4.8.1:

$$V_H = \frac{S_H l_H}{Sc} \qquad \textbf{(4.8.1)}$$

And V_V is the vertical tail volume coefficient and is given by Equation 4.8.2:

$$V_V = \frac{S_V l_V}{Sb} \qquad \textbf{(4.8.2)}$$

Both of the above equations depend heavily on the tail moment arm, specifically the distance from the tail to the aerodynamic center. A range for this value was determined to be between 0.3 and 0.65 meters.

For an overall design, the tail will utilize a flat plate in a conventional model and utilize two servos for the rudder and elevator deflection. The wires connecting these servos to the battery and other electrical components will run through the fuselage and be held down with command strips. A small landing gear wheel will also be placed at the base of the tail to satisfy the tail dragger model. The tail will not require a very strong system to secure it to the fuselage as the forces generated by the tail are minimal compared to the wings. The tail surfaces will also be covered in monokote on top of the balsa wood and glue construction. The vertical tail will be offset slightly from the horizontal tail surface to allow simultaneous movement of both control surfaces without interference. The current tail dimensions are displayed below in Table 4.8.1:

Table 4.8.1 - Tail Dimensions	
Horizontal Tail Surface	
Area S_H (cm^2)	450
Span (cm)	30
Chord (cm)	15
Vertical Tail Surface	
Area S_V (cm^2)	225
Span (cm)	22.5
Chord (cm)	10

4.9 - Landing Gear Design

The landing gear design that will be implemented for this project is the tricycle landing gear formation. The tricycle formation features a single wheel under the nose of the aircraft and pair of wheels slightly aft of the center of gravity. Tricycle gear aircraft are typically easier to take-off and land. Provided the given flying environment and past experiences with turf take-off, the tricycle system was chosen opposed to skids. The wheels to be used are that of the HBZ3100 that are made of foam. The nose gear wheel will be inserted into the balsa body of the aircraft and be fastened by the provided screws. The main landing gear that is comprised of two foam wheels attached by an aluminum rod will be attached just aft of the center of gravity. Since the main landing gear will be experiencing the majority of the load during take-off and landing, on top of the screw fasteners, some form of tape may be added to secure the rod to the underbelly of the fuselage. The driving factor of landing gear selection was payload attachment. The tricycle landing gear provides enough ground clearance that allows for the payload to situated under the aircraft which gives way to overall better aircraft performance.

4.10 - Weight and Balance

As mentioned in section 4.2, the mass of every provided part and current rocket prototype were measured and reported in Table 4.2.1, which was reposted here for convenience. This yields a total mass of 0.449 kg without water, just the electronic parts, and the current rocket prototype weight. Team Mustang is still assuming an approximate mass of 1.7 kg for the empty

plane. This accounts for the monokote, glue, balsa wood structure, screws, and 3D printed parts. When this is factored in, the total assumed mass is 2.192 kg. For the Final Design Review, a CAD version of the aircraft will be created. This will allow precision measurement of mass and more importantly - the center of gravity. Both Solidworks and Autodesk Inventor have the ability to calculate the exact center of gravity in an assembly. This will be utilized to confirm the calculated center of gravity. Computational fluid dynamics software will be utilized to confirm the aerodynamic center, specifically the CFD package in ANSYS.

Table 4.2.1 - System Parts and Masses	
Part	**Mass (g)**
Rocket Nose Cone	36.5
Rocket Fins	20
Rocket Tape	5
Rocket Parachute	6
Rocket Body	45.5
3 Control Surface Servos	76
Motor	115
Battery	95
Electronic Receiver and Transmitter	11
Landing Gear	30
Screws, Mounts, Rubber Bands	25
Total of Rocket Prototype 1 (no water)	113
Total Aircraft Components	386.5
Total Combined (without water, balsa wood)	499.5
Assumed Final Aircraft Empty Mass	1700
Total Mass with Assumed Aircraft Mass (with water)	**2192**

4.11 - Longitudinal Stability

Longitudinal stability is an absolutely critical area to focus on to maintain flight performance. Specifically, $C_{m\alpha}$ and C_{m0} equations and curves need to be created an analyzed to ensure longitudinal stability. This specifically deals with the location of the center of gravity, ensuring it is forward of the aerodynamic center. This allows the plane to pitch down in the event of a stall, and not get caught in a stall and lose control. For rectangular wings, the aerodynamic center is at the quarter chord. Therefore, the center of gravity must be placed forward of this point. The following two equations will be analyzed to determine this exact location:

$$C_{m0} = C_{m0_w} + C_{m0_f} + \eta V_H C_{L\alpha_T}(\varepsilon_0 + i_w - i_t) - \eta V_H C_{L\alpha_c}(\varepsilon_0 + i_w - i_c) \quad \textbf{(4.11.1)}$$

$$C_{m\alpha} = C_{L\alpha_w}(\tfrac{x_{cg}}{c} - \tfrac{x_{ac}}{c}) + C_{m\alpha_f} - \eta V_H C_{L\alpha_T}(1 - \tfrac{d\varepsilon}{d\alpha}) + \eta V_H C_{L\alpha_c}(1 - \tfrac{d\varepsilon}{d\alpha}) \quad \textbf{(4.11.2)}$$

Making the assumption that downwash is negligible, and that the aircraft does not have a canard, and the fuselage effects are negligible, the equations can be simplified to equations 4.11.3 and 4.11.4:

$$C_{m0} = C_{m0_w} + \eta V_H C_{L\alpha_T}(\varepsilon_0 + i_w - i_t) \quad \textbf{(4.11.3)}$$

$$C_{m\alpha} = C_{L\alpha_w}(\tfrac{x_{cg}}{c} - \tfrac{x_{ac}}{c}) - \eta V_H C_{L\alpha_T} \quad \textbf{(4.11.4)}$$

Once further determinations about the wings and tail are confirmed, these equations can be solved. This will be done by assuming the angle of attack for zero lift on a Clark Y airfoil in a low Reynolds number environment. This will then yield the moment coefficient about the airfoil, which should be similar to the moment about the aerodynamic center. With no tail incidence set, C_{m0} should also reflect a similar value. According to other R/C models at low Reynolds numbers, this is a typical expectation.

Utilizing source #11, a Clark Y airfoil at a Reynolds number of approximately 100,000 should see a moment coefficient of -0.06 at a 0 degree angle of attack, and a zero value moment coefficient at an angle of attack of -5 degrees, as seen in Figure 4.11.1. Ideally, this plot should see a negative slope for a positive alpha to show stability, as seen in Figure 4.11.2. That is the general expected plot we plan to achieve after calculating the center of gravity

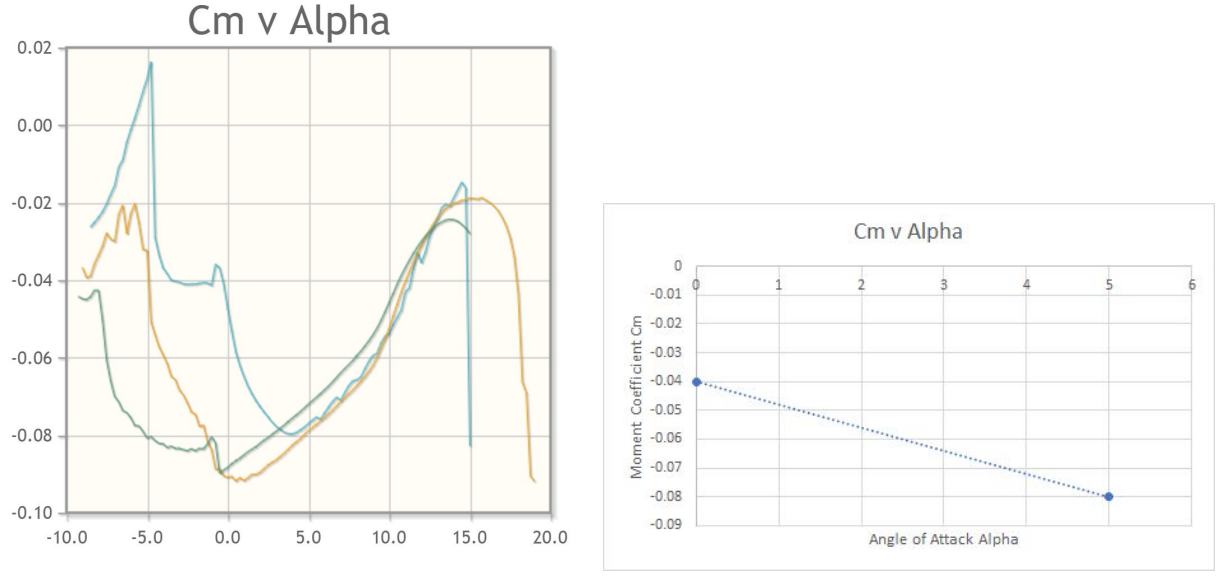

Figure 4.11.1 - Clark Y Cm v Alpha; Figure 4.11.2 - Expected Cm v Alpha

MIT and source #13 suggest a range for the stability margin ratio to be between 0.05 and 0.15. The stability margin is given by Equation 4.11.1. This will be accounted for in future optimization. Ideally, a more stable aircraft is desired in this scenario, so a much larger static margin is desirable. A smaller static margin yields a less stable but more responsive aircraft

$$S.M. = \frac{x_{np} - x_{cg}}{c} \qquad \textbf{(4.11.1)}$$

4.12 - Updated Predicted Performance

The predicted performance was recalculated utilizing all of the new inputs and assumptions. Team Mustang utilized the same method from section 3.6 and equation 3.6.1. The team's score increased by over 300% from the initial prediction which only predicted seven laps. This number was drastically low due to a battery lifespan estimation of only 120 seconds. The newly written code with the old CDR inputs predicts close to 90 laps, which would yield a score of 1350. The new predicted score of 423 is a 68% decrease from this score.

The first adjustments came from re-optimizing the amount of water in the bottle rocket, adding official coefficient of drag values for the bottle and parachute, and recalculating the full weight. This yielded a time aloft of nine seconds, a 40% decrease from the original estimation of 15 seconds aloft. This is likely due to the coefficient of drag of the parachute decreasing by nearly 50% from the original value after testing. Figure 4.12.1 shows the result of the predicted rocket performance.

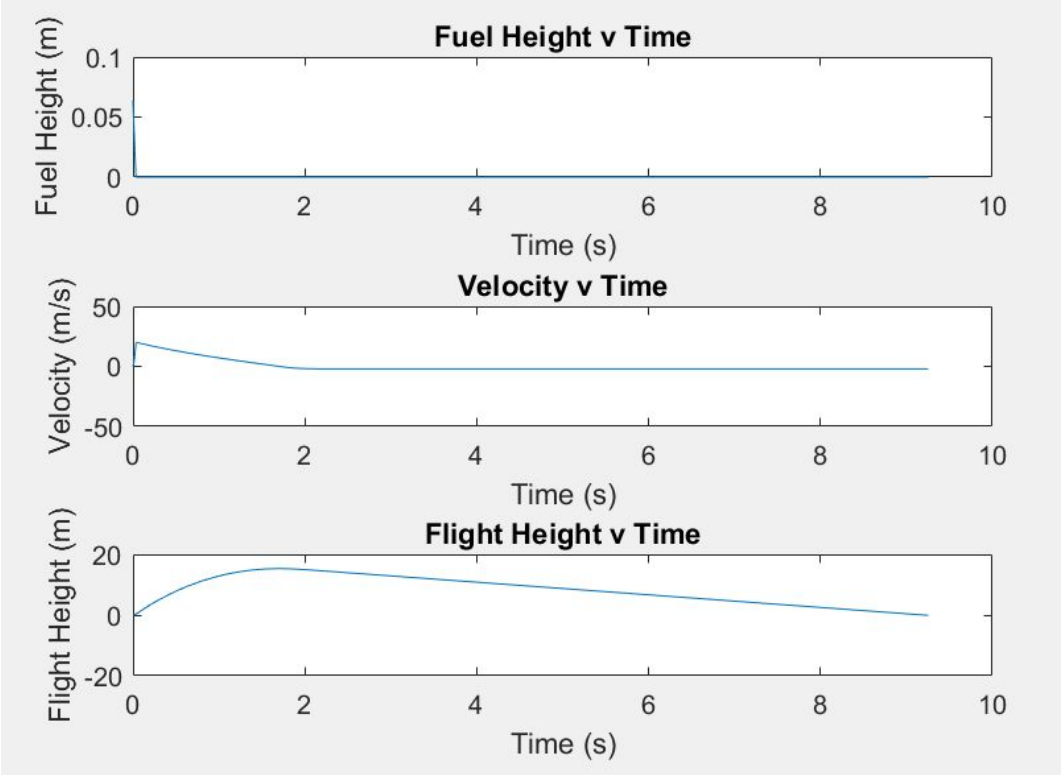

Figure 4.12.1 - Rocket Predicted Performance

The aircraft performance was also replotted and re-optimized. Figure 4.12.2 shows the current and power required plots for the new aircraft inputs at a variety of inputs. The chosen cruise

velocity of 6 meters per second lies in the initial few set of points where the slope is minimal, which is ideal for extending battery life and increasing the number of laps able to be completed.

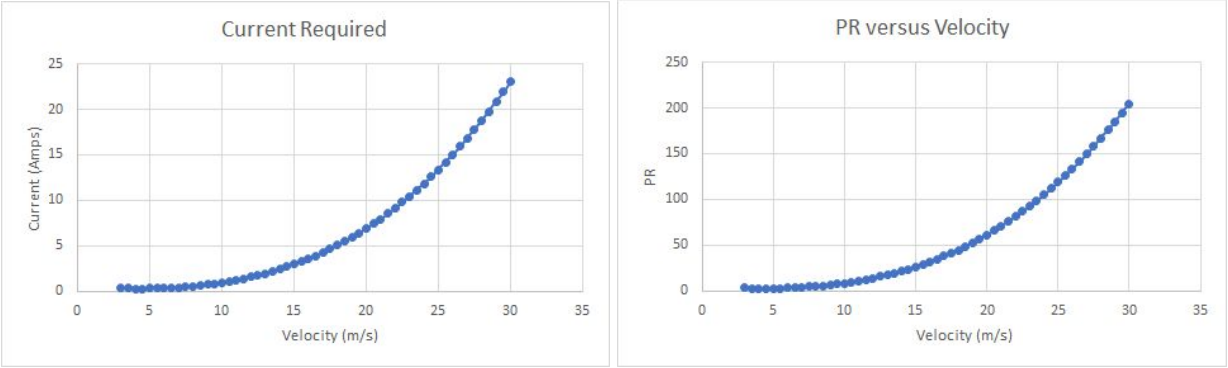

Figure 4.12.2 - Rocket Predicted Performance

The time of flight was also plotted as seen in Figure 4.12.3. This surprisingly predicts a lower cruise velocity to be optimal compared to the number of laps completed. The predicted value here is 4.5 meters per second, which is approaching the stall velocity of 3.33 meters per second. There is a rapid drop off in time of flight after this value, leading Team Mustang to reaffirm the confirmed cruise velocity of 6 meters per second, as explained in the laps completed plot of Figure 4.12.4 below.

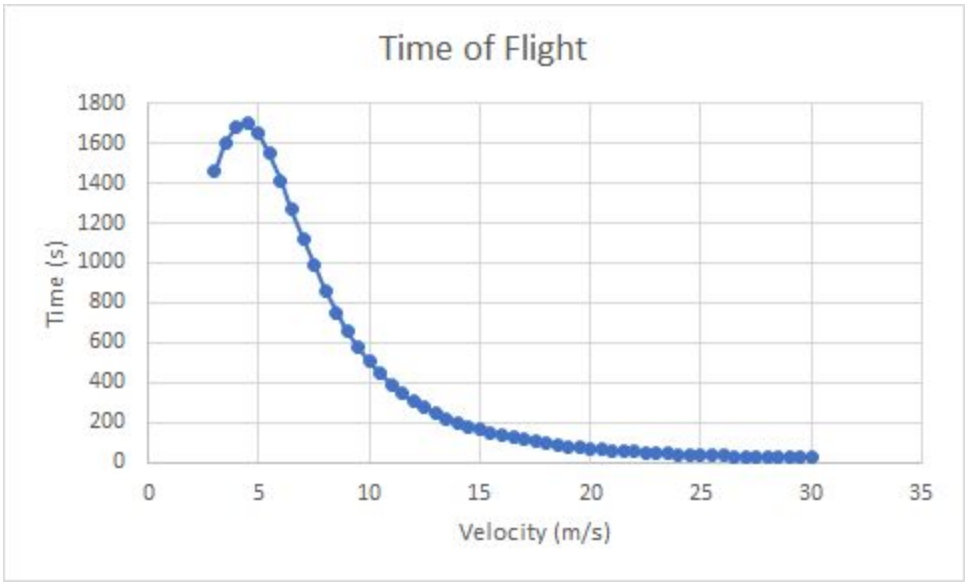

Figure 4.12.3 - Rocket Predicted Performance

Figure 4.12.4 shows the total laps completed at varying velocities. This was chosen to verify the cruise velocity of 6 meters per second because lap count is the driving design factor. This plot peaks at 6 meters per second and then sees a sharp decline in performance as the velocity

increases. This was expected, but Team Mustang had initially predicted a cruise velocity of approximately 10 meters per second. This coincides with the approximate optimal speeds described in Figures 4.12.2 and 4.12.3. This predicts just shy of 50 laps being completed, which is a great prediction for Team Mustang's score. 50 laps is a 614% increase from the original 7 lap prediction. This code will be updated for the final design review to account for takeoff and landing battery usage.

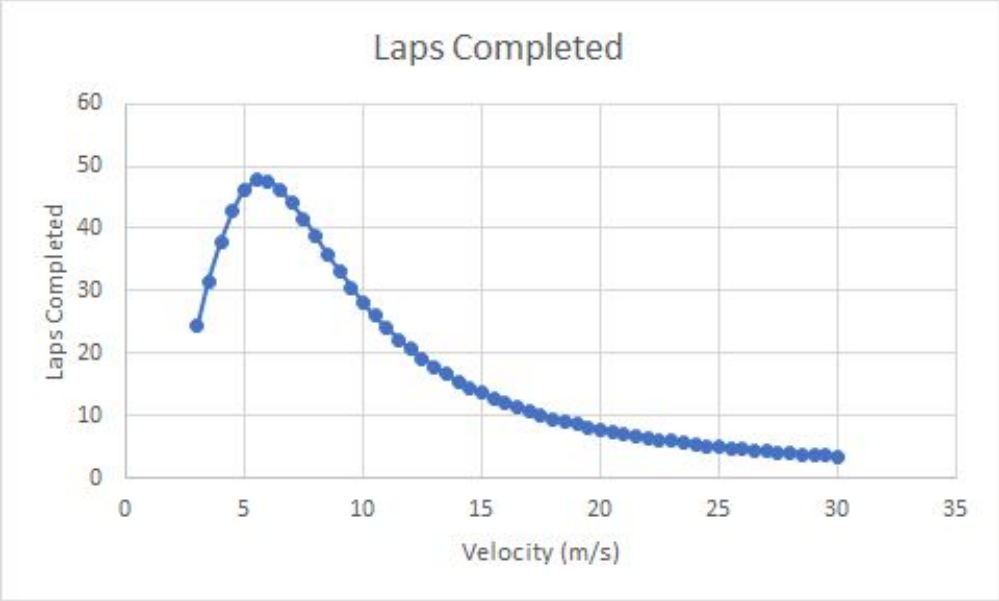

Figure 4.12.4 - Rocket Predicted Performance

To summarize the updated performance parameters, Table 4.12.1 is provided to show every finalized value appropriate to predicted performance, along with the predicted score of 423. This is again given by Equation 3.6.1 and utilizes the number of laps completed and the time aloft for the bottle rocket. Team Mustang is pleasantly surprised with these results, and although they will likely decrease when more realistic values and risks are accounted for in the final design review, this is a promising base prediction. Team Mustang would be ecstatic achieving half of the predicted 47 laps performed with an approximate total score of 200.

Table 4.12.1 - Updated Performance Parameters	
Chord (m)	0.2
Span (m)	1.25
AR	6.25
Cruise Velocity (m/s)	6
Airplane Mass (kg)	~1.7
Time of Flight (s)	~1500
Number of Laps Completed	**47**
Rocket Parachute Choice	24 inch Canvas
Rocket Parachute Cd	0.68
Rocket Weight (kg)	0.372
Percent of Water	19%
Time Aloft	**9**
Total Mass (kg)	2.192
Total Score	423

Chapter 5 - Final Design Review

5.1 - CAD Model of Aircraft

The following images show a visual representation of our aircraft, generated using SolidWorks computer-aided design. This model does not include the Monokote liner or any propulsion, electronic, control systems. This model reflects accurate materials, with the wings and tail constructed out of balsa wood, the fuselage constructed out of a thin-walled PVC tube, and the engine mount and rocket components 3D printed with PLA plastic.

This CAD model allowed for the confirmation that the center of gravity is forward of the aerodynamic center (the quarter chord for straight rectangular wings.) This model features eight custom designed and 3D printed parts. All are shown in blue. At the front of the fuselage is the motor mount, which was created at an angle to account for the torque generated by the motor spinning (as is in the original model). The rocket nose cone was redesigned to feature a completely circular body instead of a tip. The fins were also thickened and now feature a circular curve on the face attached to the body, to allow complete flushness along the body of the bottle. Lastly, the bottle will be mounted utilizing zip-ties. These will be held in place by two 3D printed motor mounts.

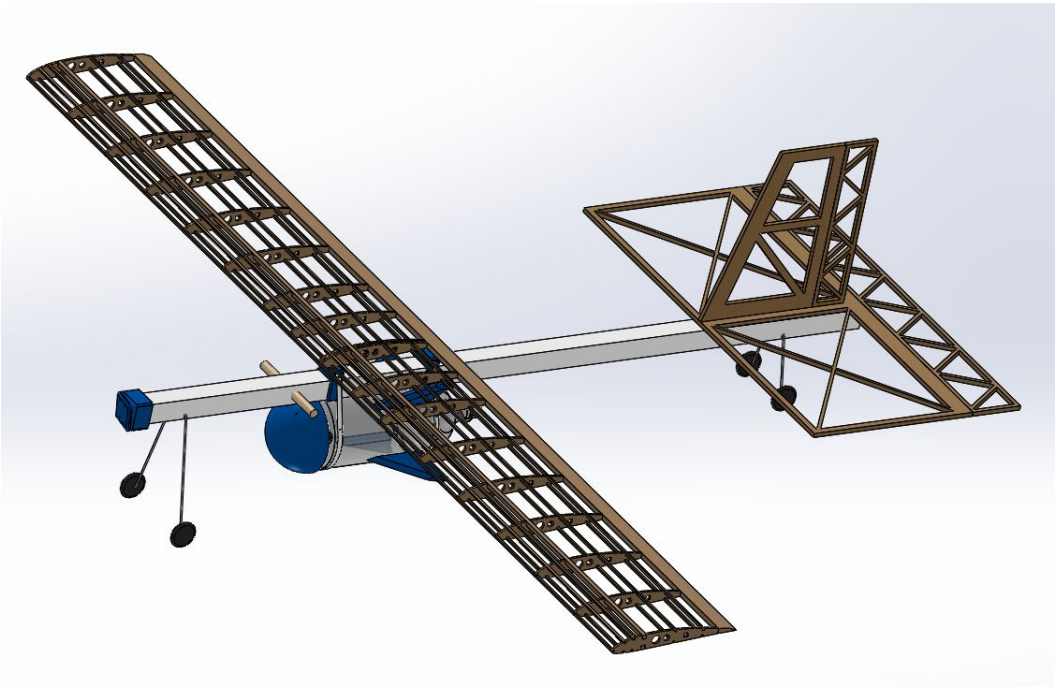

Figure 5.1.1 - 3D CAD Model: Oblique Angle

Figure 5.1.2 - 3D CAD Model: Front View

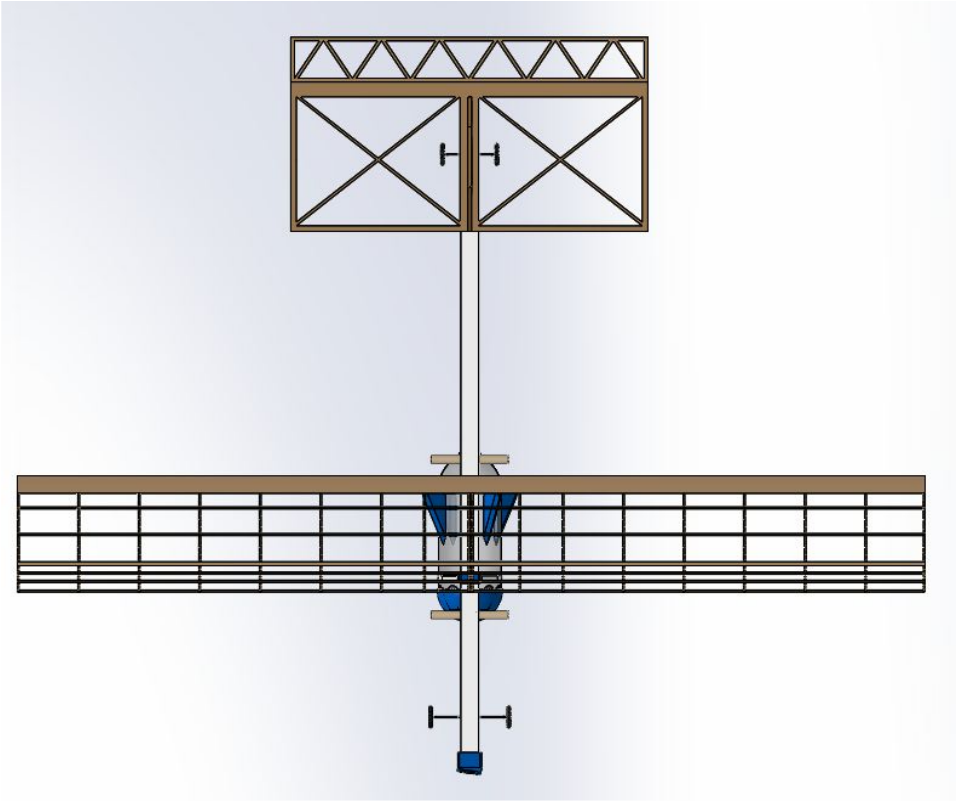

Figure 5.1.3 - 3D CAD Model: Top View

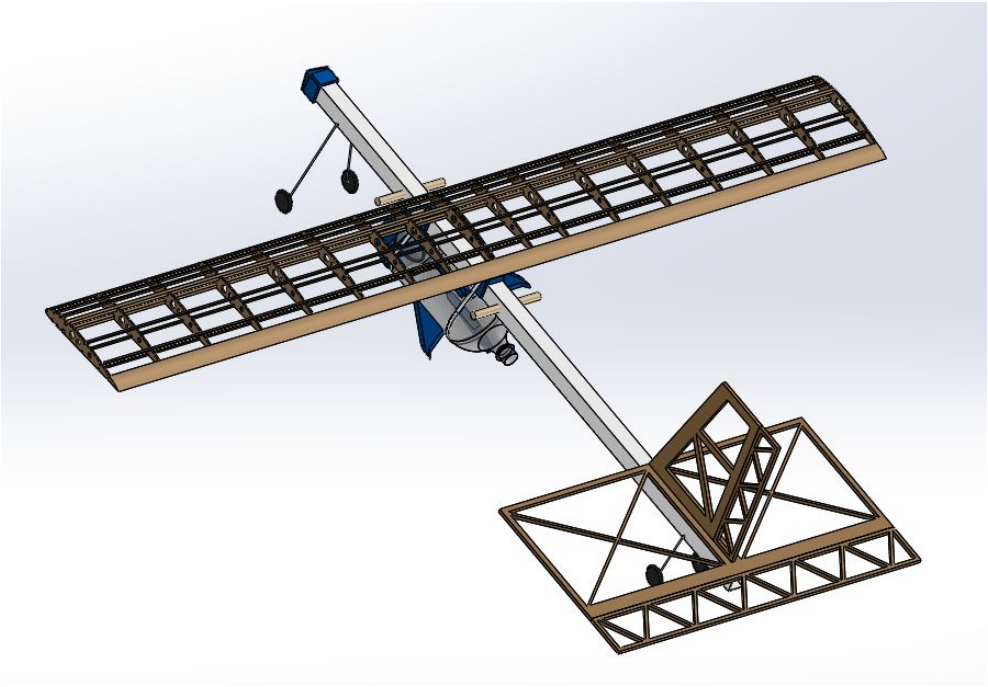

Figure 5.1.4 - 3D CAD Model: Back Angle

5.2 - Manufacturing Process

To create an efficient and effective manufacturing process with quality materials, we decided to keep a couple fundamental concepts in mind: Patience and simplicity. The manufacturing process is where a lot can go wrong if we did not do it correctly the first time. From our materials budget (Section 5.3), we see that a total of $126.91 was spent gathering materials. If we rushed the manufacturing process or attempted a complicated and confusing assembly method, our chances for aircraft success in test flights drops significantly, and a re-build would be a costly process, both financially and with respect to our time and energy.

Instead, we made the process as simple as we could while maintaining necessary precision that any aerospace system calls for. For the wing, airfoil ribs were laser cut out of balsa wood using CAD models. These airfoils included notches cut from the outer edges where two main spars and 9 stringers could be laid and glued using purple cyanoacrylate (CA) adhesive. There were also lightening holes cut from the ribs to lower the weight of our aircraft while still maintaining a strong structural capability. The rocket will be assembled separately before being attached. The fins will be attached utilizing command strips and tape, with the nose cone taped down during flight to hold the parachute down. In the rocket flight, the nose cone will not be secured. A balloon will be inserted to prevent water sloshing and secured internally with a bottle cap. Before the wing is attached, wires and electronics will be glued and installed throughout the fuselage. Then the motor and motor mount will be glued into place. Following installation of the dowels, the wing will be installed, and finally the tail. Before all of this happens, appropriate

holes will be drilled in the fuselage for both electrical wiring passages and weight reduction at the aft of the fuselage (to assist with a more forward center of gravity). The wing features nine stringers and two spars, as seen in the images in sections 5.1 and 5.2. More ribs are included in the center to provide increased structural integrity along the fuselage. The goal with this wing system is to create two or three wings to utilize in the event of catastrophic failure, with easy installation featuring the rubber bands.

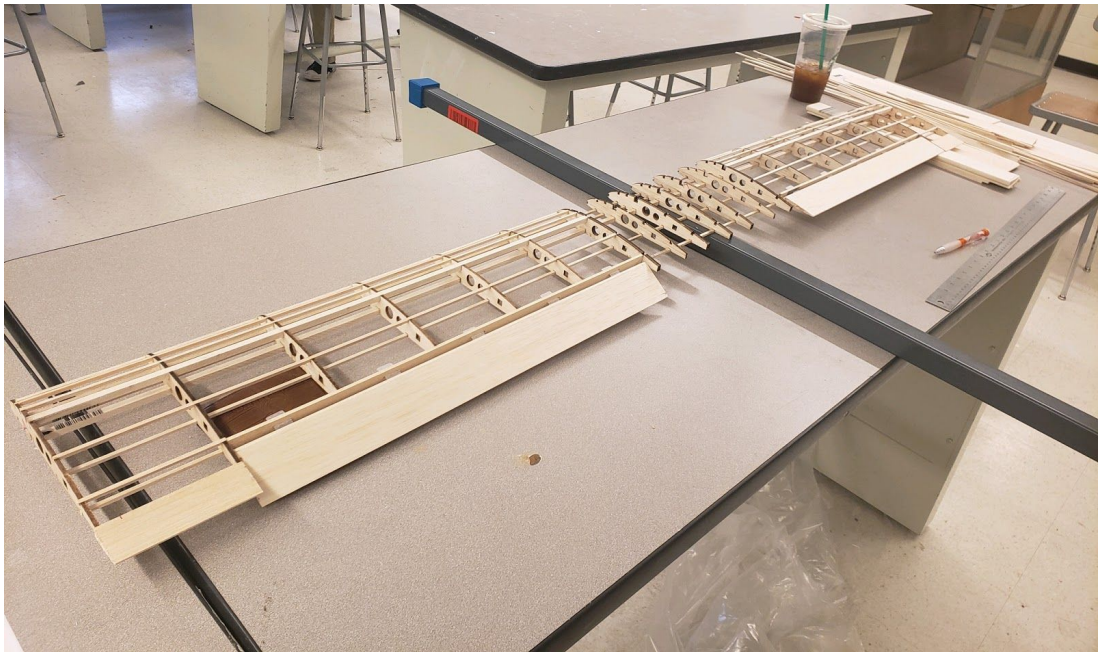

Figure 5.2.1 - Fully Assembled Wing

The wing is to be covered in a Monokote film using a heat iron and gun. The Monokoting process will be practiced on a small piece of wing built for practice before being applied to our actual wing. This will increase our experience and lessen the likelihood of making a mistake while applying Monokote to our final wing. Monokote will also be applied to our vertical and horizontal tail sections, which will be built using ⅜” x ⅜” balsa sticks and combined using CA adhesive.

Our fuselage consists of a ¾” x ¾” x 48” rod of square PVC pipe, which will hold all of our assembly together. The propulsion system will be secured using space-filling CA glue to the “nose” of the PVC pipe. The wiring will be strung inside the hollow PVC pipe and leading to the control systems for the wing and tail. Holes will be drilled through the PVC where necessary to allow wiring to exit and connect to the control systems. The wing will be mounted on the fuselage using rubber bands wrapped diagonally across the center of the wing and connected to dowels protruding from the fuselage. The tail section will be connected using space-filling CA adhesive at the rear of the fuselage. Our landing gear will be held in place by cutting small notches in the fuselage and fitting the wire bar connecting the wheels into the notch, then

fastening it in place with space-filling CA adhesive. All control systems will be connected using space-filling CA adhesive to ensure strong bonds and light weight. Finally, our bottle rocket will be secured to our aircraft using large, thick zip ties held in place longitudinally by space-filling CA adhesive.

With this easy manufacturing process in mind, every part is easily replaceable in the event of catastrophic failure. The fuselage was picked to prevent any failure and provide immense structural integrity. Every part along the fuselage can easily be replaced or resecured if necessary.

5.3 - Budget

To determine our total financial contributions to our aircraft, we used a spreadsheet calculator that included item, quantity and cost to add our total projected total from the items we purchased. A picture of this spreadsheet can be seen below:

Senior Design Budget																			
Team Mustang																			
Walt's Hobby						**Amazon**													
Trip 1						**Order 1**													
Supplies	**Qty.**		**Cost**			**Supplies**	**Qty.**		**Cost**										
BC Sanding Stick	1		1.99			1-3/16 x 1-3/16 x 48 PVC	1		17.06										
BC Lightduty Knife	1		3.49																
Nylon Parachute 24in	1		10.49			Subtotal			17.06										
Blue CA glue	1		5.99			Tax			1.36										
1/8 x 6 x 36 Balsa Sheet	4		15.96			Total			18.42										
1/4 x 1/4 x 36 Balsa Stick	6		2.94																
1/8 x 1/8 x 36 Balsa Stick	26		7.00																
Subtotal			47.86																
Tax			4.39														**Project Total:**		126.91
Total			52.25																
Trip 2																			
Supplies	**Qty.**		**Cost**																
1/8 x 1/2 x 36 Balsa Stick	2		0.98																
5/16 x 1-1/4 x 36 Balsa TR	1		1.49																
3/8 x 2 x 36 Balsa Aileron	2		5.38																
Purple CA Glue	1		3.99																
Hinge Nylon	15		6.25																
Monokote 6'	2		33.98																
Subtotal			52.07																
Tax			4.17																
Total			56.24																

Figure 5.3.1 - Budget Spreadsheet

5.4 - Operational Plan (Flight and Ground Handling)

After much consideration and deliberation, Mike Aiello has been selected to pilot our aircraft during our final flight demonstration. Mike has the most experience flying RC aircraft, and is the most familiar with the control system provided.

To prepare for the operation of our home-made aircraft, Mike will first practice using the control system on the HBZ 3100. This will refresh Mike's knowledge of the control system and provide a stable platform for re-learning the controls. From there, we will proceed to disassemble the HBZ 3100 and attach the control systems to our aircraft. Before we take our hard work to the

skies, we will hold the plane stationary and test all electronics in a controlled and risk-free setting to make sure all parts work as expected. Next, we will take to the Carrier Dome.

One of our biggest goals is to be able to take off our aircraft from the ground, so we will be testing our airplane with our bottle rocket attached and weighted. First we will attempt to achieve SLUF just a couple feet off the ground. The next flight we will test the pitch of our aircraft angling the nose up and down to test ability to change altitude. When we feel comfortable controlling pitch, we will move to banking maneuvers, starting gradual and slowly steepening the radius of curvature. Finally, we will attempt to put it all together and attempt to complete the design requirement: figure 8 maneuvers across the entire football field. These test flights will take place both on our own time and during the provided shake-down flight time.

This crawl-walk-run methodology to flight and ground handling will maximize our confidence flying our aircraft by minimizing the risk we are taking into intervals. This way, if a crash does happen, it happens under our controlled conditions, and any damages can be prepared for. This method may sound slow and tedious, but it is also steady and careful, minimizing potential time being wasted making large repairs after catastrophic crashes due to rushing the operational process.

5.5 - Expected Performance

From our most recent numbers and parameters set or our aircraft, we expect our aircraft to weigh a total of 975 grams, and our rocket to weigh 550.51g including water. This adds to a total weight of 1525.51 grams that will need to be lifted off the ground.

Updating our performance code yielded a total of 20 laps expected to be completed by our aircraft, and a rocket time aloft of 6 seconds. In total, our expected score for the project is expected to be 120 points. Below, figure 5.5.1 shows the updated performance with the new parameters, and figure 4.12.1 shows the original laps flown with regard to cruise velocity. It is acknowledged that predicting the number of laps based off of cruise velocity is difficult as the velocity will likely vary. However, the predicted number of laps of 20 now agrees with the predicted performance shown in Figure 4.3.1 when utilizing the updated weight and new span and chord parameters. This figure again calculates the laps flown based off of the chord and span.

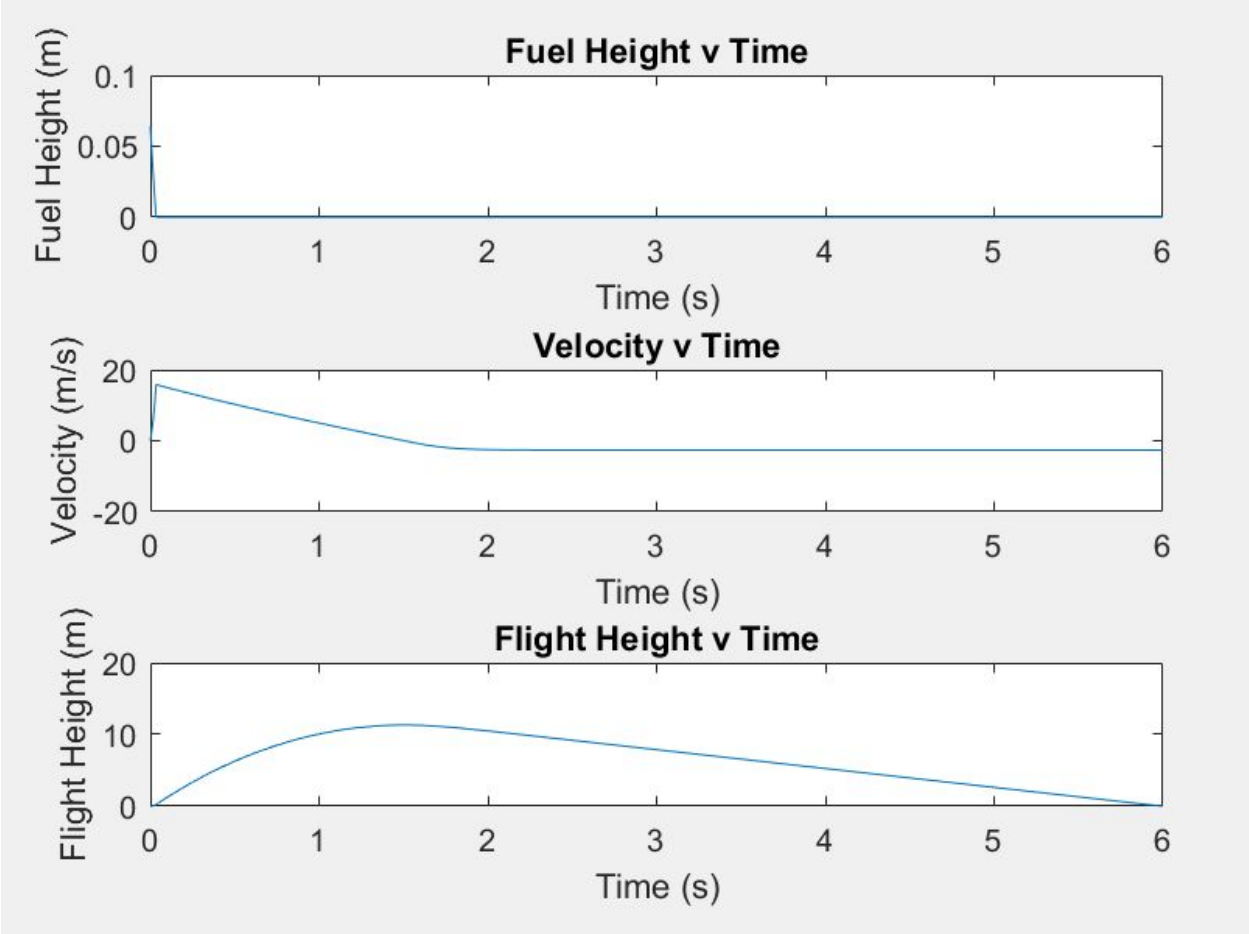

Figure 5.5.1 - Updated Performance

Appendix A: Bibliography

1. "Cartoon-Plane." *CAF Red Tail Squadron*. Web. <www.redtail.org/cartoon-plane/>
2. "Easy Sky Drifter" *JRCModel.com*. Web. <http://www.jrcmodel.com/store/p23/EasySky_Drifter_Ultralight_2.4G_4Ch_ES9908_Electric_RC_Plane_950mm_EPO.html>
3. "Eppler E210" *Airfoil Tools*. Web. <http://airfoiltools.com/airfoil/details?airfoil=e210-il#polars>
4. "Football: The Field" *Ducksters.com*. Web. <https://www.ducksters.com/sports/football/field_dimensions.php>
5. "Hornet Micro RC Plane" *Hobbyking.com*. Web. <https://hobbyking.com/en_us/micro-plane-oem-sticker-design-mode-2.html>
6. "Mini Apprentice F RTS" *Hobbyzone.com*. Web. <https://www.hobbyzone.com/rc-airplanes/trainers/hobbyzone/HBZ3100.html>
7. "Model Aircraft" *AeroModelBasic.* Web. <http://aeromodelbasic.blogspot.com/2011/09/x-gliders-exploring-flight-research.html>
8. "NACA 2412" *Airfoil Tools.* Web. <http://airfoiltools.com/airfoil/details?airfoil=naca2412-il#polars>
9. "Rolling Coefficients" *HPWizard.com*. Web. <http://hpwizard.com/tire-friction-coefficient.html>
10. "Selig S1223" *Airfoil Tools.* Web. <http://airfoiltools.com/airfoil/details?airfoil=s1223-il#polars>
11. "Clark Y Airfoil" *Airfoil Tools.* Web. <http://airfoiltools.com/airfoil/details?airfoil=clarky-il>
12. "Pitching Moment" *Wikipedia*. Web. <https://en.wikipedia.org/wiki/Pitching_moment>
13. "Lab 8 Notes - Basic Aircraft Design Rules" *MIT.* Web. <https://ocw.mit.edu/courses/aeronautics-and-astronautics/16-01-unified-engineering-i-ii-iii-iv-fall-2005-spring-2006/systems-labs-06/spl8.pdf>

Appendix B: MATLAB Code

Rocket code

```
% Team Mustang
% Bottle Rocket Simulation
% Michael Aiello

clc
clear all

% Fuel height
h_initial = 0.06384; %m

% Velocity
V_initial = 0;

% Height
y_initial = 0;

% Call Function
[t,xyz] = ode45(@ode45fun,[0 30], [h_initial V_initial y_initial]);

terminal_landing = find(xyz(:,3)< 0,1);

hh = xyz(:,1);
VV = xyz(:,2);
yy = xyz(:,3);

% Plots
figure
subplot(3,1,1)
plot(t(1:terminal_landing),hh(1:terminal_landing))
title 'Fuel Height v Time'
xlabel 'Time (s)'
ylabel 'Fuel Height (m)'
hold on
subplot(3,1,2)
plot(t(1:terminal_landing),VV(1:terminal_landing))
title 'Velocity v Time'
xlabel 'Time (s)'
```

```
ylabel 'Velocity (m/s)'
hold on
subplot(3,1,3)
plot(t(1:terminal_landing),yy(1:terminal_landing))
title 'Flight Height v Time'
xlabel 'Time (s)'
ylabel 'Flight Height (m)'

% Function Integrator
function [states] = ode45fun(t,xyz)
h = xyz(1);
V = xyz(2);
y = xyz(3);

if h < 0
   h = 0;
end

% Input Measurments
h_initial = 0.06384;
CD = 0.45;
rho = 1.225; %kg/m^3
R = 0.05075; %m
m_empty = 0.112; %kg
rho_h2o = 1000; %kg/m^3
H = .336; %m
g = 9.81; %m/s^2
P_initial = 344738; %Pa
CDSC = 0.84;
Pinf = 101325; %Pa
r = .02; %m

% Drag Equation
Drag = CD.*.5.*rho.*(abs(V).*V).*(pi.*(R.^2));

if V < 0
   CD = .68;
   ParaArea = .6096; %24inches to m
   Drag = CD.*.5.*rho.*(abs(V).*V).*(ParaArea);
end

% Rocket Weight
m = m_empty + rho_h2o.*h.*(pi.*(R.^2));
```

```
Weight = m.*g;

% Components of Thrust Equation
Ptank = (P_initial.*(H - h_initial))./(H - h);

if h == 0
   Ptank = Pinf;
end

Pn = Ptank + rho_h2o.*g.*h;

Vn = CDSC.*(sqrt((Pn-Pinf)./(rho_h2o)));
m_dot = rho_h2o.*Vn.*(pi.*(r.^2));

% Thrust Equation
Thrust = Vn.*m_dot;

% States
states = zeros(size(xyz));
states(1) = -m_dot./(rho_h2o.*(pi.*(R.^2)));
states(2) = (Thrust - Drag - Weight)./m;
states(3) = V;

end
```

Airplane code

```
% Team Mustang
% Airplane Simulation
% Michael Aiello

% Airplane Characteristics
% Flight time (12-15mins)
W = 2.192; %kg                          % weight
S = 0.25; %m^2                          % wing area
b = 1.25; %m                            % span
AR = (b.^2)./S;                         % aspect ratio
CDo = 0.0500;                           % parasite drag
e = 0.8;                                % oswald effeciency
CLmax = 1.0;                            % max lift coefficient
rho = 1.225; %kg/m^3 (sea level)        % density
V_cruise = 13; %m/s                     % cruise velocity
```

```
Imax = 18;                          % max current draw
Iavg = 10;                          % average current draw
motor_eff = 0.22;                   % motor efficiency
CDroll = 0.25;                      % roll coefficent
BatteryEff = 0.25;                  % battery efficiency
wingheight = 0.35; %m               % wing height from ground
phi = ((16*wingheight/b).^2)...
   /(1+(16*wingheight/b).^2);       % ground effect
newtonW = (W.*9.81); %N             % weight in newtons
volt = 11.1;                        % batttery power

% SLUF
V_stall = sqrt((2.*newtonW)...
   ./(rho.*S.*CLmax)); %m/s         % stall velocity
V = linspace((V_stall+0.001),15,100); %m/s     % velocity range
q = .5.*rho.*(V.^2);                % dynamic pressure

Lift = CLmax.*q.*S; %N              % lift

CL = newtonW./(.5.*rho.*(V.^2).*S);          % lift coefficient
CD = CDo + (((CL.^2)./(pi.*e.*AR)));         % drag coefficient
TR = CD.*q.*S; %N                   % thrust required

PR = ((TR.*V)./volt)./BatteryEff; %watts     % power required (amperage)
PA = 45; %watts                     % power available

RoC = (PA-PR)./newtonW; %m/s        % rate of climb
D = CD.*q.*S; %N                    % drag
V_LO = 0.7*1.2.*V_stall; %m/s       % liftoff velocity
V_T = 0.7*1.3.*V_stall; %m/s        % landing velocity

T = PA./(V_LO); %N                  % thrust


% Takeoff
LO_CL = newtonW./(.5.*rho.*(V_LO.^2).*S);
LO_CD = CDo + (phi.*((LO_CL.^2)./(pi.*e.*AR)));
LO_L = LO_CL.*q.*S;
LO_D = LO_CD.*q.*S;

% Friction Coefficient
% Assuming Dome Turf is some combination of grass and gravel
Turf = 0.575;
```

```
S_LO = (1.44*(newtonW.^2))./(32.2.*rho.*S.*CLmax.*...
   (T-(LO_D+Turf.*(newtonW-LO_L))));

% Landing
t_CL = newtonW./(.5.*rho.*(V_T.^2).*S);
t_CD = CDo + (phi.*((CL.^2)./(pi.*e.*AR)));
t_L = t_CL.*q.*S;
t_D = t_CD.*q.*S;

S_L = (1.69*(newtonW.^2))./(32.2.*rho.*S.*CLmax.*...
   (t_D+Turf.*(newtonW-t_L)).*(0.7.*V_T));

% Turning
g = 9.81; %m/s
eta = (.5.*rho.*(V.^2).*CLmax)./(newtonW./S);
R = (V.^2)./(g.*(sqrt((eta.^2)-1)));
omega = (g.*(sqrt((eta.^2)-1)))./V;


% Flight Performance
length = 60;
d = 2.*pi.*R +(sqrt((length.^2) + ((2.*R).^2)));
laptime = d./V;
batterytime = (1137./(PR.*10.^3)).*3600; %s
LapNum = batterytime./laptime;

% Array Index locator
bestflight = find(LapNum>max(LapNum)-0.00001, 1)


% Performance Plots

% Plot TR v V
figure
hold on
plot(V,TR)
title('TR vs. V')
xlabel('Velocity (m/s)')
ylabel('Thrust Required (N)')


% Plot CL v V
figure
```

```
hold on
plot(V,CL)
title('CL vs. V')
xlabel('Velocity (m/s)')
ylabel('Coefficient of Lift')


% Plot PR v V
figure
hold on
plot(V, PR)
title('PR vs. V')
xlabel('Velocity (m/s)')
ylabel('Power Required (watts)')
```